Frequency Selective Heteronuclear Dipolar Recoupling in Rotating Solids: Accurate $^{13}C-^{15}N$ Distance Measurements in Uniformly $^{13}C,^{15}N$-labeled Peptides

Christopher P. Jaroniec,[†] Brett A. Tounge,[†,§] Judith Herzfeld,[§] and Robert G. Griffin*,[†]

Contribution from the Department of Chemistry and Francis Bitter Magnet Laboratory, Massachusetts Institute of Technology, Cambridge, Massachusetts 02139, and Department of Chemistry and Keck Institute for Cellular Visualization, Brandeis University, Waltham, Massachusetts 02454-9110

Received September 5, 2000. Revised Manuscript Received January 24, 2001

Abstract: We describe a magic-angle spinning NMR experiment for selective $^{13}C-^{15}N$ distance measurements in uniformly $^{13}C,^{15}N$-labeled solids, where multiple $^{13}C-^{15}N$ and $^{13}C-^{13}C$ interactions complicate the accurate measurement of structurally interesting, weak $^{13}C-^{15}N$ dipolar couplings. The new experiment, termed FSR (*f*requency *s*elective *R*EDOR), combines the REDOR pulse sequence with a frequency selective spin−echo to recouple a single $^{13}C-^{15}N$ dipolar interaction in a multiple spin system. Concurrently the remaining $^{13}C-^{15}N$ dipolar couplings and all $^{13}C-^{13}C$ scalar couplings to the selected ^{13}C are suppressed. The $^{13}C-^{15}N$ coupling of interest is extracted by a least-squares fit of the experimentally observed modulation of the ^{13}C spin−echo intensity to the analytical expression describing the dipolar dephasing in an isolated heteronuclear spin pair under conventional REDOR. The experiment is demonstrated in three uniformly $^{13}C,^{15}N$-labeled model systems: asparagine, *N*-acetyl-L-Val-L-Leu and *N*-formyl-L-Met-L-Leu-L-Phe; in *N*-formyl-[U-$^{13}C,^{15}N$]L-Met-L-Leu-L-Phe we have determined a total of 16 internuclear distances in the 2.5−6 Å range.

Introduction

Solid-state nuclear magnetic resonance (SSNMR) experiments designed to measure dipolar couplings are very important in structural investigations of biological systems,[1−3] which are not amenable to X-ray diffraction or solution-state NMR methods.[4−6] Such systems include membrane proteins,[1,3,7−11] large enzyme−inhibitor complexes,[12,13] chemical and photochemical reaction intermediates,[9,11,14] peptide−protein complexes,[15] and peptide aggregates.[16−22] In particular, the accurate measurement of $^{13}C-^{13}C$ and $^{13}C-^{15}N$ dipolar couplings corresponding to internuclear distances in the 3−6 Å range can provide detailed information about the three-dimensional structure of biological solids.

The resolution and sensitivity of SSNMR experiments are optimized by the combination of high static magnetic fields ($B_0 \geq \sim$11.7 T) with (i) macroscopic orientation of the sample with respect to the external field[3] or (ii) rapid rotation of the sample about an axis tilted away from B_0 by the "magic-angle", $\theta = \tan^{-1}\sqrt{2}$. In the case of magic-angle spinning (MAS),[23,24] the high resolution is achieved at the expense of structural informa-

* To whom correspondence should be addressed. E-mail: rgg@mit.edu.
† Massachusetts Institute of Technology.
§ Brandeis University.

(1) Griffin, R. G. *Nat. Struct. Biol.* **1998**, *5*, 508−512.
(2) McDowell, L. M.; Schaefer, J. *Curr. Opin. Struct. Biol.* **1996**, *6*, 624−629.
(3) Opella, S. J. *Nat. Struct. Biol.* **1997**, *4*, 845−848.
(4) McRee, D. E. *Practical Protein Crystallography*; Academic Press: San Diego, 1993.
(5) Saenger, W. *Principles of Nucleic Acid Structure*; Springer-Verlag: New York, 1984.
(6) Wüthrich, K. *NMR of Proteins and Nucleic Acids*; Wiley: New York, 1986.
(7) Creuzet, F.; McDermott, A.; Gebhard, R.; van der Hoef, K.; Spijker-Assink, M. B.; Herzfeld, J.; Lugtenburg, J.; Levitt, M. H.; Griffin, R. G. *Science* **1991**, *251*, 783−786.
(8) Thompson, L. K.; McDermott, A. E.; Raap, J.; van der Wielen, C. M.; Lugtenburg, J.; Herzfeld, J.; Griffin, R. G. *Biochemistry* **1992**, *31*, 7931−7938.
(9) Lakshmi, K. V.; Auger, M.; Raap, J.; Lugtenburg, J.; Griffin, R. G.; Herzfeld, J. *J. Am. Chem. Soc.* **1993**, *115*, 8515−8516.
(10) Feng, X.; Verdegem, P. J. E.; Lee, Y. K.; Sandström, D.; Edén, M.; Bovee-Geurts, P.; de Grip, W. J.; Lugtenburg, J.; de Groot, H. J. M.; Levitt, M. H. *J. Am. Chem. Soc.* **1997**, *119*, 6853−6857.
(11) Griffiths, J. M.; Bennett, A. E.; Engelhard, M.; Siebert, F.; Raap, J.; Lugtenburg, J.; Herzfeld, J.; Griffin, R. G. *Biochemistry* **2000**, *39*, 362−371.
(12) McDermott, A. E.; Creuzet, F.; Griffin, R. G.; Zawadzke, L. E.; Ye, Q. Z.; Walsh, C. T. *Biochemistry* **1990**, *29*, 5767.
(13) McDowell, L. M.; Schmidt, A.; Cohen, E. R.; Studelska, D. R.; Schaefer, J. *J. Mol. Biol.* **1996**, *256*, 160−171.

(14) Li, Y.; Appleyard, R. J.; Shuttleworth, W. A.; Evans, J. N. S. *J. Am. Chem. Soc.* **1994**, *116*, 10799−10800.
(15) Weliky, D. P.; Bennett, A. E.; Zvi, A.; Anglister, J.; Steinbach, P. J.; Tycko, R. *Nat. Struct. Biol.* **1999**, *6*, 141−145.
(16) Spencer, R. G. S.; Halverson, K. J.; Auger, M.; McDermott, A. E.; Griffin, R. G.; Lansbury, P. T. *Biochemistry* **1991**, *30*, 10382−10387.
(17) Griffiths, J. M.; Ashburn, T. T.; Auger, M.; Costa, P. R.; Griffin, R. G.; Lansbury, P. T. *J. Am. Chem. Soc.* **1995**, *117*, 3539−3546.
(18) Lansbury, P. T.; Costa, P. R.; Griffiths, J. M.; Simon, E. J.; Auger, M.; Halverson, K. J.; Kocisko, D. A.; Hendsch, Z. S.; Ashburn, T. T.; Spencer, R. G. S.; Tidor, B.; Griffin, R. G. *Nat. Struct. Biol.* **1995**, *2*, 990−998.
(19) Benzinger, T. L. S.; Gregory, D. M.; Burkoth, T. S.; Miller-Auer, H.; Lynn, D. G.; Botto, R. E.; Meredith, S. C. *Proc. Natl. Acad. Sci. U.S.A.* **1998**, *95*, 13407−13412.
(20) Gregory, D. M.; Benzinger, T. L. S.; Burkoth, T. S.; Miller-Auer, H.; Lynn, D. G.; Meredith, S. C.; Botto, R. E. *Solid State Nucl. Magn. Reson.* **1998**, *13*, 149−166.
(21) Benzinger, T. L. S.; Gregory, D. M.; Burkoth, T. S.; Miller-Auer, H.; Lynn, D. G.; Botto, R. E.; Meredith, S. C. *Biochemistry* **2000**, *39*, 3491−3499.
(22) Antzutkin, O. N.; Balbach, J. J.; Leapman, R. D.; Rizzo, N. W.; Reed, J.; Tycko, R. *Proc. Natl. Acad. Sci. U.S.A.* **2000**, *97*, 13045−13050. Balbach, J. J.; Ishii, Y.; Antzutkin, O. N.; Leapman, R. D.; Rizzo, N. W.; Dyda, F.; Reed, J.; Tycko, R. *Biochemistry* **2000**, *39*, 13748−13759. Tycko, R. *Curr. Opin. Chem. Biol.* **2000**, *4*, 500−506.
(23) Andrew, E. R.; Bradbury, A.; Eades, R. G. *Nature* **1958**, *182*, 1659.
(24) Lowe, I. J. *Phys. Rev. Lett.* **1959**, *2*, 285.

tion, as MAS effectively attenuates the dipolar couplings between low-γ nuclei, such as ^{13}C and ^{15}N. However, the fact that spin components of the dipolar Hamiltonian can be manipulated using radio frequency (rf) pulses allows dipolar couplings to be reintroduced into the spin dynamics using pulse sequences designed to interfere with the spatial modulation of the dipolar interaction due to MAS.

Various homonuclear and heteronuclear dipolar recoupling techniques have been developed and applied to distance measurements in pairs of spin-$^1/_2$ nuclei, determination of relative orientations of dipolar tensors, and polarization transfer in chemical shift correlation experiments. Most of the existing recoupling experiments including a number of applications have been reviewed in detail.[1,25,26] Here we focus our attention on accurate ^{13}C$-^{15}$N distance measurements in uniformly ^{13}C,^{15}N-labeled biomolecules.

The recoupling of isolated low-γ heteronuclear spin pairs can be accomplished using windowless techniques such as cross-polarization (CP)[27] or rotary resonance recoupling (R^3)[28,29] and related experiments,[30] as well as pulsed methods based on rotational-echo double-resonance (REDOR).[31,32] Typically, REDOR experiments employ phase-alternated π pulse schemes (e.g., xy-4, xy-8, etc.)[33] to compensate for pulse imperfections and resonance offsets,[34] and can provide ^{13}C$-^{15}$N distances up to ~6 Å.[2,26] Furthermore, for sequences based on xy-4, finite pulse effects are relatively minor[35] making REDOR compatible with the high MAS frequencies ($\omega_r/2\pi \approx 10-20$ kHz) required for high-field studies of U-^{13}C,^{15}N-labeled systems with strong ^{1}H couplings.

Although experiments which probe heteronuclear distances in isolated spin pairs continue to provide valuable structural information, there is a compelling motivation for developing SSNMR techniques for distance measurements in larger spin systems, where multiple internuclear distances can be determined. In particular, such techniques provide a means to circumvent the time-consuming and laborious preparation of multiple specifically labeled samples. Instead, a single multiply labeled sample will suffice. However, the application of methods developed for spin pairs to distance measurements in U-^{13}C,^{15}N-labeled systems is generally not straightforward, due to the presence of multiple homonuclear and heteronuclear spin$-$spin interactions. This is particularly exacerbated for weak heteronuclear couplings, which provide the most useful information about the three-dimensional arrangement of nuclei in the system. For example, it is well-known that REDOR dipolar dephasing of a single S spin by multiple I spins in an I_nS spin system depends on the magnitudes and relative orientations of all dipolar

couplings.[36-39] (The situation is analogous for heteronuclear $I-S$ correlation experiments[40,41] based on transferred-echo double-resonance (TEDOR),[42] where cross-peak intensities depend on multiple couplings.) In the simplest multispin system of this type (I_2S), the dephasing profile is most sensitive to changes in spin topology when the two $I-S$ interactions have similar magnitude and the I_1-S-I_2 angle, θ_{12}, is close to 0° or 180°.[39] (Similar observations have also been made in a number of dipolar tensor correlation experiments designed to measure bond and dihedral angles.[30,43-47]) However, in general, when the size and approximate geometry of the spin system are completely unknown, the accurate measurement of weak couplings in the presence of stronger ones becomes problematic.[39]

Several modified versions of REDOR have been developed to overcome the dependence of dipolar dephasing curves in coupled spin clusters on multiple couplings and their relative orientations. θ-REDOR[48] encodes the information about all $I-S$ couplings into the observable S spin signal in an I_nS system, while eliminating the dependence on the relative orientation of the interactions. Although θ-REDOR is very useful for reporting simultaneously on all dipolar couplings present in the multiple spin system, the extension of this method to the accurate measurement of weak couplings in uniformly ^{13}C,^{15}N-labeled peptides is not straightforward. For this particular task, frequency selective methods appear to be more generally applicable. An example of this approach is frequency selective dipolar recoupling (FDR),[49,50] where rotor-synchronized π pulses (one per rotor period) are applied to the observed S (^{13}C) nuclei, and $\pi/2$ pulses[49] or a combination of $\pi/2$ and π pulses[50] are applied to the I (^{15}N) spins. The FDR pulse sequence generates a dipolar Hamiltonian similar to REDOR, but with an important modification: the I-spin resonance offset, δ_I, is explicitly encoded into the spin dynamics. For on-resonance I nuclei ($\delta_I = 0$) the Hamiltonian is purely dipolar, and when $\delta_I \gg b_{IS}$ (where b_{IS} is the $I-S$ dipolar coupling constant), the dipolar dephasing is quenched. The FDR method was demonstrated in several model multispin systems including [1,4-^{13}C, 1,2-^{15}N]Gly-Gly·HCl,[50] where all four ^{13}C$-^{15}$N dipolar couplings were measured (in particular the 20 Hz C$_4-$N$_1$ coupling corresponding to ~5.4 Å distance could be observed in the presence of the ~200 Hz C$_4-$N$_2$ coupling).

(25) Bennett, A. E.; Griffin, R. G.; Vega, S. In *Solid State NMR IV: Methods and Applications of Solid-State NMR*; Blumich, B., Ed.; Springer-Verlag: Berlin, 1994; Vol. 33, pp 1−77.

(26) Dusold, S.; Sebald, A. *Annu. Rep. Nucl. Magn. Reson. Spectrosc.* **2000**, *41*, 185−264.

(27) Pines, A.; Gibby, M. G.; Waugh, J. S. *J. Chem. Phys.* **1973**, *59*, 569−590.

(28) Oas, T. G.; Griffin, R. G.; Levitt, M. H. *J. Chem. Phys.* **1988**, *89*, 692−695.

(29) Levitt, M. H.; Oas, T. G.; Griffin, R. G. *Isr. J. Chem.* **1988**, *28*, 271−282.

(30) Costa, P. R.; Gross, J. D.; Hong, M.; Griffin, R. G. *Chem. Phys. Lett.* **1997**, *280*, 95−103.

(31) Gullion, T.; Schaefer, J. *J. Magn. Reson.* **1989**, *81*, 196−200.

(32) Gullion, T.; Schaefer, J. *Adv. Magn. Reson.* **1989**, *13*, 57−83.

(33) Gullion, T.; Baker, D. B.; Conradi, M. S. *J. Magn. Reson.* **1990**, *89*, 479−484.

(34) Gullion, T.; Schaefer, J. *J. Magn. Reson.* **1991**, *92*, 439−442.

(35) Jaroniec, C. P.; Tounge, B. A.; Rienstra, C. M.; Herzfeld, J.; Griffin, R. G. *J. Magn. Reson.* **2000**, *146*, 132−139.

(36) Fyfe, C. A.; Lewis, A. R.; Chézeau, J. M.; Grondey, H. *J. Am. Chem. Soc.* **1997**, *119*, 12210−12222.

(37) Goetz, J. M.; Schaefer, J. *J. Magn. Reson.* **1997**, *127*, 147−154.

(38) Nishimura, K.; Naito, A.; Tuzi, S.; Saito, H. *J. Phys. Chem. B* **1999**, *103*, 8398−8404.

(39) Fyfe, C. A.; Lewis, A. R. *J. Phys. Chem. B* **2000**, *104*, 48−55.

(40) van Eck, E. R. H.; Veeman, W. S. *J. Magn. Reson. A* **1994**, *109*, 250−252.

(41) Michal, C. A.; Jelinski, L. W. *J. Am. Chem. Soc.* **1997**, *119*, 9059−9060.

(42) Hing, A. W.; Vega, S.; Schaefer, J. *J. Magn. Reson.* **1992**, *96*, 205−209.

(43) Feng, X.; Lee, Y. K.; Sandström, D.; Eden, M.; Maisel, H.; Sebald, A.; Levitt, M. H. *Chem. Phys. Lett.* **1996**, *257*, 314−320.

(44) Hong, M.; Gross, J. D.; Griffin, R. G. *J. Phys. Chem. B* **1997**, *101*, 5869−5874.

(45) Feng, X.; Eden, M.; Brinkmann, A.; Luthman, H.; Eriksson, L.; Gräslund, A.; Antzutkin, O. N.; Levitt, M. H. *J. Am. Chem. Soc.* **1997**, *119*, 12006−12007.

(46) Hohwy, M.; Jaroniec, C. P.; Reif, B.; Rienstra, C. M.; Griffin, R. G. *J. Am. Chem. Soc.* **2000**, *122*, 3218−3219.

(47) Reif, B.; Hohwy, M.; Jaroniec, C. P.; Rienstra, C. M.; Griffin, R. G. *J. Magn. Reson.* **2000**, *145*, 132−141.

(48) Gullion, T.; Pennington, C. H. *Chem. Phys. Lett.* **1998**, *290*, 88−93. Liivak, O.; Zax, D. B. *J. Chem. Phys.* **2000**, *113*, 1088−1096.

(49) Bennett, A. E.; Becerra, L. R.; Griffin, R. G. *J. Chem. Phys.* **1994**, *100*, 812−814.

(50) Bennett, A. E.; Rienstra, C. M.; Lansbury, P. T.; Griffin, R. G. *J. Chem. Phys.* **1996**, *105*, 10289−10299.

Complications can arise when applying FDR (and other REDOR experiments) to U-^{13}C,^{15}N-labeled systems. The π-pulse train on the ^{13}C channel would recouple the ^{13}C nuclei,[51] create unwanted coherences, and therefore fail to simply and cleanly recouple ^{13}C$-^{15}$N pairs. The irradiation of the ^{15}N nuclei, however, does not suffer from such an effect since in peptides the dipolar coupling strengths go in the order ^{13}C$-^{13}$C (2 kHz) $\gg$ ^{15}N$-^{15}$N (50 Hz), and amide ^{15}N resonances exhibit a relatively small chemical dispersion. The accurate measurement of weak ^{13}C$-^{15}$N couplings ($b_{CN} \approx 20-100$ Hz) corresponding to distances in the $3-6$ Å range is further complicated by ^{13}C$-^{13}$C scalar couplings since the dipolar evolution time is limited to approximately $(2J_{CC})^{-1}$ ($\sim 10-15$ ms in peptides, where one-bond ^{13}C$-^{13}$C J couplings are in the $30-60$ Hz range[52]).

We have recently described a *J*-decoupled REDOR experiment,[53] which suppresses ^{13}C$-^{13}$C scalar couplings and enables the measurement of weak dipolar couplings between a single ^{15}N nucleus and individual ^{13}C nuclei within a coupled cluster. In that experiment the homonuclear *J* couplings, assumed to be in the weak-coupling limit ($H_J = 2\pi J_{12}S_{1z}S_{2z}$),[54] are refocused by a frequency selective spin-echo,[55] realized in practice by applying a frequency selective π pulse to a single ^{13}C spin. (Homonuclear *J* decoupling of this type has also been used for resolution enhancement in two-dimensional correlation spectroscopy.[56,57]) The basic principle of using frequency selective spin-echoes to retain certain interactions while refocusing others can be extended to include heteronuclear dipolar couplings. Here we describe a selective recoupling experiment based on this idea and termed FSR (*f*requency *s*elective *R*EDOR), which combines REDOR with a frequency selective spin-echo generated by a pair of frequency selective π pulses applied to a ^{13}C$-^{15}$N spin pair in the multispin system. We note that although in our implementation we use REDOR ($H_D \propto I_z S_z$) to achieve broadband recoupling, in principle, other sequences, which generate an analogous effective dipolar Hamiltonian (e.g., SPI-R^3)[30] could also be used. For multiple ^{13}C,^{15}N spin systems with sufficient ^{13}C and ^{15}N chemical shift dispersion, the application of the FSR pulse sequence generates an observable ^{13}C signal, which depends on a single ^{13}C$-^{15}$N dipolar coupling; the remaining ^{13}C$-^{15}$N interactions and all ^{13}C$-^{13}$C scalar couplings involving the selected ^{13}C are suppressed. The dipolar coupling of interest is extracted by fitting the modulation of the ^{13}C spin-echo to the analytical expression describing dipolar dephasing in an isolated heteronuclear spin pair under conventional REDOR.[32] We demonstrate the utility of the FSR experiment by measuring a number of structurally interesting internuclear distances in U-^{13}C,^{15}N-labeled peptides, *N*-acetyl-L-Val-L-Leu and *N*-formyl-L-Met-L-Leu-L-Phe; for the latter peptide a total of 16 distances in the $2.5-6$ Å regime were determined, with a precision in the range $0.1-0.3$ Å.

(51) Gullion, T.; Vega, S. *Chem. Phys. Lett.* **1992**, *194*, 423−428. Bennett, A. E.; Ok, J. H.; Griffin, R. G.; Vega, S. *J. Chem. Phys.* **1992**, *96*, 8624−8627.

(52) Cavanagh, J.; Fairbrother, W. J.; Palmer, A. G.; Skelton, N. J. *Protein NMR Spectroscopy: Principles and Practice*; Academic Press: San Diego, 1996.

(53) Jaroniec, C. P.; Tounge, B. A.; Rienstra, C. M.; Herzfeld, J.; Griffin, R. G. *J. Am. Chem. Soc.* **1999**, *121*, 10237−10238.

(54) Ernst, R. R.; Bodenhausen, G.; Wokaun, A. *Principles of Nuclear Magnetic Resonance in One and Two Dimensions*; Clarendon Press: Oxford, 1991.

(55) Hahn, E. L. *Phys. Rev.* **1950**, *80*, 580.

(56) Brüschweiler, R.; Griesinger, C.; Sørensen, O. W.; Ernst, R. R. *J. Magn. Reson.* **1988**, *78*, 178−185.

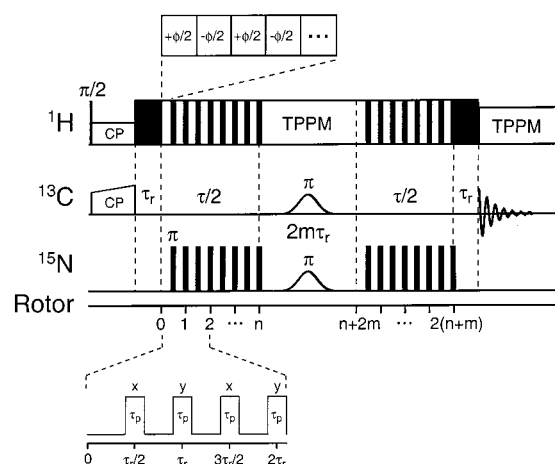(57) Straus, S. K.; Bremi, T.; Ernst, R. R. *Chem. Phys. Lett.* **1996**, *262*, 709−715.

Figure 1. Frequency selective REDOR (FSR) pulse sequence. Following ramped cross-polarization[27,58] from ^{1}H to ^{13}C the ^{13}C$-^{15}$N dipolar couplings are reintroduced via a REDOR[31,32] sequence. The frequency selective recoupling of ^{13}C$-^{15}$N spin pairs is achieved by the generation of a ^{13}C spin−echo using a pair of rotor-synchronized frequency selective π pulses applied simultaneously on the ^{13}C and ^{15}N channels (the frequency of the ^{15}N selective pulse is independent of the REDOR π pulses). Couplings to protons during the ^{13}C$-^{15}$N dipolar recoupling period are attenuated using a combination of CW and TPPM[59] decoupling, represented by filled and hollow rectangles, respectively. To account for the relaxation of spin coherences, a reference (S_0) experiment is recorded for each dipolar dephasing (S) experiment, by acquiring the ^{13}C spin−echo in the absence of the selective ^{15}N pulse, which results in the refocusing of all ^{15}N dipolar couplings to the selected ^{13}C.

Experimental Section

NMR Experiments. NMR spectra were recorded at 11.7 T (500.1 MHz ^{1}H, 125.8 MHz ^{13}C, 50.7 MHz ^{15}N) using a custom-designed spectrometer (courtesy of Dr. David J. Ruben) with a custom-designed quadruple-resonance MAS probe and a Chemagnetics (Fort Collins, CO) triple-resonance MAS probe. The probes were equipped with 4.0 mm Chemagnetics spinning modules. Spinning frequencies of 10.0 or 12.5 kHz were used in all experiments and regulated to ±5 Hz with a Doty Scientific (Columbia, SC) spinning frequency controller. Samples were centerpacked in the rotors to minimize the effects of rf inhomogeneity (measured to be $\sim 5-10\%$ fwhm using the standard nutation method[80]).

The FSR pulse sequence is presented in Figure 1. Ramped cross-polarization[27,58] from ^{1}H creates the initial ^{13}C magnetization. Subsequently, a REDOR pulse sequence[31,32] is initiated for time $\tau/2 = n\tau_r$ to recouple the ^{13}C$-^{15}$N dipolar interactions in a nonselective fashion. All rotor-synchronized π pulses (timing shown in inset) are applied on the ^{15}N channel to avoid the recoupling of ^{13}C spins[51] and phased according to the $xy-4$ scheme[33] to compensate for pulse imperfections and resonance offsets.

The frequency selective spin−echo is generated by the application of simultaneous rotor-synchronized selective π pulses on the ^{13}C and ^{15}N channels, where the frequency of the ^{15}N pulse can be varied independently of the REDOR π pulses. Selective irradiation accomplishes the following: (i) signals originating from ^{13}C nuclei not affected by the ^{13}C selective pulse are eliminated by phase cycling ($\phi_{Gauss} = xy\overline{xy}$, $\phi_{rec'r} = x\overline{x}x\overline{x}$), (ii) all ^{13}C$-^{13}$C scalar couplings to the selected ^{13}C are suppressed,[53] and (iii) the ^{13}C spin−echo intensity is modulated only by ^{13}C$-^{15}$N dipolar couplings to the ^{15}N nuclei irradiated by the selective pulse, while the dipolar couplings to the nonirradiated ^{15}N are refocused. In our implementation, we use Gaussian pulses on both channels, timed such that their maxima coincide with the midpoint of the selective irradiation period occupying an even number of rotor cycles

(58) Metz, G.; Wu, X.; Smith, S. O. *J. Magn. Reson. A* **1994**, *110*, 219−227.

$(2m\tau_r)$. Selective pulses were calibrated using the pulse sequence:

$$CP_x - (\pi/2)_y - z\text{-filter} - \tau_{\text{Gauss}} - z\text{-filter} - (\pi/2) - \text{acquire}$$

where τ_{Gauss} was fixed at a constant value while the amplitude of the pulse was increased resulting in the nutation of the observable magnetization (a π pulse corresponds to maximum inversion).

Following the selective irradiation period, a REDOR pulse sequence, identical to that applied prior to the selective pulses, is initiated for time $\tau/2 = n\tau_r$. During this period, dipolar couplings involving the selected $^{13}C-^{15}N$ spin pairs are retained, while $^{13}C-^{13}C$ scalar couplings and remaining $^{13}C-^{15}N$ dipolar couplings are refocused. Additional delays of τ_r, during which no dipolar evolution occurs, are inserted following CP and immediately before signal acquisition. The purpose of the second delay is to avoid the acquisition of the ^{13}C FID during ^{15}N rf irradiation; the delay following CP preserves the symmetry of the sequence. The influence of proton couplings during the $^{13}C-^{15}N$ recoupling period is attenuated by a combination of resonant continuous-wave (CW) and two-pulse phase modulation (TPPM)[59] decoupling (see Results and Discussion Section for details). TPPM decoupling was used during acquisition.

Unless otherwise indicated, the ^{15}N REDOR π pulse length was 18 μs ($\omega_{rf}/2\pi \approx 28$ kHz), the TPPM ^1H decoupling was ∼120 kHz ($\phi = 15°$, $\tau = 4.0$ μs), the CW decoupling was 125 kHz, and the ^{13}C and ^{15}N Gaussian pulses were 1.0−5.0 ms and 1.0−10.0 ms, respectively. Each selective pulse was divided into 64−512 increments, and the Gaussian profile was truncated at 1% of the maximum amplitude.

Internuclear Distance Measurements. During the FSR pulse sequence the information about a single $^{13}C-^{15}N$ dipolar coupling is encoded into the observable signal intensity. Therefore, the dipolar coupling constant of interest can be extracted by fitting the experimentally observed modulation of the ^{13}C spin−echo intensity to the analytical expression describing the dipolar dephasing in an isolated heteronuclear spin pair under conventional REDOR:[32]

$$\Delta S/S_0(\tau) = \lambda[1 - \langle\cos(\omega_{CN}\tau)\rangle] \qquad (1)$$

$\Delta S/S_0 = 1 - S/S_0$, where S_0 and S represent the reference and dipolar dephasing experiments, respectively (cf. Figure 1). The dipolar coupling, ω_{CN}, is a function of the $^{13}C-^{15}N$ dipolar coupling constant, b_{CN}, and $\langle\cdots\rangle$ represents the average over random orientations of the dipole vector in the powder sample (see Theoretical Background section for details). The scaling factor, λ, accounts for the contribution to S_0 from ^{13}C spins without a neighboring ^{15}N, which is the result of imperfect isotopic labeling and dilution of the labeled compound with natural abundance material.

In the FSR experiment, λ also accounts for a small scaling of the dipolar dephasing amplitude resulting from the imperfect inversion of ^{15}N spin coherences by the ^{15}N selective pulse and decay of coherences due to insufficient ^1H decoupling during the selective pulse. The amplitude scaling was found to be negligible for 1−10 ms ^{15}N selective pulses when recoupling ^{15}N with small chemical shielding anisotropy (CSA) and small effective $^{15}N-^1H$ coupling (e.g., NH_3^+ groups under the experimental conditions employed in this work) (data not shown). For ^{15}N nuclei with larger CSA and $^{15}N-^1H$ coupling (e.g., amide groups) the scaling was also negligible for short (∼1 ms) ^{15}N selective pulses. However, for pulses in the 6−10 ms range the dephasing amplitude had to be scaled down by ∼5−10% to accurately simulate experimental data. For most systems, internal references are available, in the form of strong $^{13}C-^{15}N$ dipolar couplings which exhibit several oscillations during typical mixing times, and λ can be easily calibrated. For example, in the U-$^{13}C,^{15}N$-labeled peptides investigated in this work, which were not diluted in natural abundance material, we expect $\lambda \approx 1.0$ for conventional REDOR. However, we find that FSR experiments for ∼200 Hz $^{13}C-^{15}N$ couplings (e.g., Val(C$^\beta$)-Val(N) in *N*-acetyl-L-Val-L-Leu), which employed 10 ms ^{15}N selective pulses, are best-fit with $\lambda \approx 0.90-0.95$. For each experiment designed to measure a single $^{13}C-^{15}N$ distance, the reduced χ^2, $\chi_\nu^2 \propto \sum_i w_i(s_{\exp}^i - s_{\sim}^i)$,[60] was

minimized by adjusting the dipolar coupling constant, b_{CN}, and amplitude scaling factor, λ, where b_{CN} was varied freely and λ was allowed to vary only within a narrow range (determined from the data for strong $^{13}C-^{15}N$ couplings). The uncertainties in b_{CN} (reported at 95% confidence level) were obtained according to the procedure described in ref 60. First, the best-fit dipolar coupling, b_{CN}^*, is determined with $\chi_{\nu,\min}^2$. Subsequently, several trial b_{CN} values are selected around b_{CN}^*, and experimental data are re-fit by optimizing λ within the previously defined range. The b_{CN} values, for which the condition $\chi_{\nu,\max}^2 = F(\nu)\chi_{\nu,\min}^2$ is satisfied ($F(\nu)$ is a constant, which depends on the number of degrees of freedom, ν, and the desired confidence level), represent the uncertainties in the best-fit dipolar coupling constant. The internuclear C−N distances, r_{CN}, are related to the dipolar coupling constants via eq 6 below (see Theoretical Background section for details).

$^{13}C,^{15}N$-Labeled Model Systems. The model compounds used in the experiments were: [1-$^{13}C,^{15}N$]glycine, [acetyl-1,2-$^{13}C,^{15}N$]*N*-acetylvaline (NAV), [U-$^{13}C,^{15}N$]asparagine, [U-$^{13}C,^{15}N$]*N*-acetyl-L-Val-L-Leu (VL) and *N*-formyl-[U-$^{13}C,^{15}N$]L-Met-L-Leu-L-Phe (MLF). All $^{13}C,^{15}N$-labeled amino acids and [1,2-^{13}C]acetic anhydride were purchased from Cambridge Isotope Laboratories (Andover, MA). VL and MLF were synthesized by Synpep (Dublin, CA) and American Peptide (Sunnyvale, CA), respectively, using standard solid-phase methods and purified by HPLC. Prior to the NMR experiments glycine, asparagine, and NAV were diluted to ∼10% in respective natural abundance compounds and recrystallized by slow evaporation of aqueous solutions. VL was crystallized from a 1:1 (v/v) H_2O:acetone solution[61] and we confirmed using X-ray crystallography (courtesy of W. Davis) that the crystal structure is in good agreement with the published structure.[62] The recrystallization of *N*-formyl-L-Met-L-Leu-L-Phe from 2-propanol results in microcrystals, which are not of sufficiently high quality for X-ray crystallography. However, an X-ray structure has been reported for the methyl ester analogue of MLF, *N*-formyl-L-Met-L-Leu-L-Phe-*O*-methyl (MLF-OMe).[63] The inspection of VL and MLF-OMe crystal structures indicates that intermolecular $^{13}C-^{15}N$ couplings are expected to have a relatively minor effect on the structurally interesting side chain-to-backbone $^{13}C-^{15}N$ distances in the 3−4 Å range in these peptides (see Supporting Information). Therefore, initial FSR experiments were performed on peptides not diluted in natural abundance compounds. However, for measurements of intramolecular distances in the 4−6 Å regime a MLF sample was prepared by diluting *N*-formyl-[U-$^{13}C,^{15}N$]L-Met-L-Leu-L-Phe to ∼10% in the natural abundance peptide followed by recrystallization from 2-propanol.

Theoretical Background

Broadband Recoupling in Multispin Systems. We consider a coupled multiple spin system consisting of n ^{13}C spins and m ^{15}N spins. In the rapid spinning regime the first-order effective Hamiltonian[64,65] describing the spin−spin couplings during the REDOR π-pulse train (Figure 1) can be written:[32]

$$H = \sum_{i=1}^{n}\sum_{j=1}^{m}\omega_{C_iN_j}2C_{iz}N_{jz} + \sum_{i<j}\pi J_{C_iC_j}2C_{iz}C_{jz} \qquad (2)$$

The C and N operators represent ^{13}C and ^{15}N spins, respectively, and $J_{C_iC_j}$ is the C_i-C_j scalar coupling constant. For ^{15}N π pulses of finite length and phase-alternated according to $xy-4$ (or

(59) Bennett, A. E.; Rienstra, C. M.; Auger, M.; Lakshmi, K. V.; Griffin, R. G. *J. Chem. Phys.* **1995**, *103*, 6951−6957.

(60) Shoemaker, D. P.; Garland, C. W.; Nibler, J. W. *Experiments in Physical Chemistry*; McGraw-Hill: New York, 1989 and references therein.

(61) Stewart, P. L.; Tycko, R.; Opella, S. J. *J. Chem. Soc., Faraday Trans. 1* **1988**, *84*, 3803−3819.

(62) Carroll, P. J.; Stewart, P. L.; Opella, S. J. *Acta Crystallogr.* **1990**, *C46*, 243−246.

(63) Gavuzzo, E.; Mazza, F.; Pochetti, G.; Scatturin, A. *Int. J. Pept. Protein Res.* **1989**, *34*, 409−415.

(64) Haeberlen, U.; Waugh, J. S. *Phys. Rev.* **1968**, *175*, 453−467.

(65) Haeberlen, U. *High-Resolution NMR in Solids: Selective Averaging*; Academic Press: New York, 1976. We use the notation, where the leading term of the Magnus expansion is indexed with one.

extensions thereof),[33] the dipolar coupling coefficients have the form:[35]

$$\omega_{C_iN_j} = -\frac{4}{\pi}\frac{\cos\left(\frac{\pi}{2}\varphi\right)}{1-\varphi^2}\,\text{Im}\{\omega_{C_iN_j}^{(1)}(\Omega_{PR}^{ij})\} \tag{3}$$

where the fraction of the rotor period, τ_r, occupied by π pulses of length τ_p is defined as

$$\varphi = \frac{2\tau_p}{\tau_r} \tag{4}$$

The Fourier component rotating at ω_r in the MAS Hamiltonian for the dipolar coupling is given by:[66]

$$\omega_{C_iN_j}^{(1)}(\Omega_{PR}^{ij}) = -b_{C_iN_j}\{\sum_{m=-2}^{2}D_{0,m}^{(2)}(\Omega_{PC}^{ij})D_{m,-1}^{(2)}(\Omega_{CR})\}d_{-1,0}^{(2)}(\beta_{RL}) \tag{5}$$

where the $C_i - N_j$ dipolar coupling constant:

$$b_{C_iN_j} = -\frac{\mu_0}{4\pi}\frac{\gamma_C\gamma_N\hbar}{r_{C_iN_j}^3} \tag{6}$$

is a function of the gyromagnetic ratios, γ_C and γ_N, of the coupled spins and the $C_i - N_j$ internuclear distance, $r_{C_iN_j}$. The Wigner rotation matrices, $D_{0,m}^{(2)}(\Omega_{PC}^{ij})$, $\Omega_{PC}^{ij} = \{0,\beta_{PC}^{ij},\gamma_{PC}^{ij}\}$, describe the transformations of individual $C_i - N_j$ dipole vectors from their principal axis systems (P^{ij}) to a common crystallite-fixed frame (C). The subsequent transformation of all crystallites in the powder sample into the rotor-fixed frame (R) is described by $D_{m,-1}^{(2)}(\Omega_{CR})$, and the reduced rotation matrix, $d_{-1,0}^{(2)}(\beta_{RL})$, transforms the rotor-fixed frame into the laboratory frame (L) via a rotation by the magic angle, $\beta_{RL} = \tan^{-1}\sqrt{2}$. In the case of a single $C - N$ dipolar coupling, for which the principal axis system coincides with the crystallite-fixed frame (i.e., $\Omega_{PC} = \{0,0,0\}$), eq 5 becomes:

$$\omega_{CN}^{(1)}(\Omega_{PR}) = \frac{b_{CN}}{2\sqrt{2}}\sin(2\beta_{PR})\,e^{i\gamma_{PR}} \tag{7}$$

and the expression for ω_{CN} (cf. eqs 2 and 3) simplifies to:

$$\omega_{CN} = -\frac{\sqrt{2}}{\pi}\frac{\cos\left(\frac{\pi}{2}\varphi\right)}{1-\varphi^2}\,b_{CN}\sin(2\beta_{PR})\sin(\gamma_{PR}) \tag{8}$$

Equation 8 differs from the expression for ideal δ-pulse REDOR[32] only by the factor $\cos(\varphi\pi/2)/(1-\varphi^2)$, which describes the finite pulse effects.[35]

The initial transverse ^{13}C density matrix created by cross-polarization[27] from ^{1}H can be written:

$$\rho(\tau_0) = \sum_i p_i C_{ix} \tag{9}$$

where p_i represents the starting polarization on the ith ^{13}C spin. In the absence of relaxation, the density matrix for individual crystallites evolves under the effective Hamiltonian in eq 2 according to:[54]

(66) Mehring, M. *Principles of High-Resolution NMR in Solids*; Springer-Verlag: Berlin, 1983.

$$\rho(\tau) = U(\tau)\rho(\tau_0)U(\tau)^{-1} \tag{10}$$

with

$$U(\tau) = \prod_{i,j}\exp\{-i\omega_{C_iN_j}\tau 2C_{iz}N_{jz}\} \times$$
$$\prod_{i<j}\exp\{-i\pi J_{C_iC_j}\tau 2C_{iz}C_{jz}\} \tag{11}$$

Explicit calculation yields

$$\rho(\tau) = \sum_i\{p_iC_{ix}\prod_j\cos(\omega_{C_iN_j}\tau)\prod_{j\neq i}\cos(\pi J_{C_iC_j}\tau)\} + ..., \tag{12}$$

where only the part of $\rho(\tau)$ corresponding to observable coherences is given. The resulting ^{13}C spin−echo intensity is:

$$S(\tau) = \langle\text{tr}\{(\sum_i C_i^+)\rho(\tau)\}\rangle = \langle\sum_i\{\tilde{p}_i\prod_j\cos(\omega_{C_iN_j}\tau) \times$$
$$\prod_{j\neq i}\cos(\pi J_{C_iC_j}\tau)\}\rangle \tag{13}$$

where coefficients $\tilde{p}_i$ include the appropriate normalization constants and $\langle\cdots\rangle$ denotes the average over the Euler angles, $\Omega_{CR} = \{\alpha_{CR},\beta_{CR},\gamma_{CR}\}$, which define random crystallites in the powder sample. Equation 13 provides the well-known result:[36−39] for Hamiltonians of the form given in eq 2, the observable coherences evolve simultaneously as products of cosine terms describing all spin−spin couplings in the multispin system, and the dependence of the observable signal on the relative orientations of all dipolar couplings is encoded in the frequencies, $\omega_{C_iN_j}$. As a result of the dependence on multiple couplings and their relative orientations, the accurate measurement of weak heteronuclear dipolar couplings in multispin systems of unknown topology is very difficult.[39]

Selective Recoupling in Multispin Systems. The effective spin−spin coupling Hamiltonian of eq 2 is a sum of commuting bilinear terms, which, in principle, can be refocused by spin−echo[55] techniques. Consider the pulse sequence of the type shown in Figure 1, where simultaneous rf irradiation on ^{13}C and ^{15}N channels is bracketed by two identical dipolar evolution periods of duration $\tau/2$. Assuming that a pair of ideal π pulses is applied in a frequency selective fashion to spins C_k and N_l in the multispin cluster the propagator for the entire pulse sequence can be written:

$$U(\tau) = \exp\{-iH(\tau/2)\}\exp\{-i\pi C_{kx}\}\exp\{-i\pi N_{lx}\} \times$$
$$\exp\{-iH(\tau/2)\} \tag{14}$$

H can be expressed as a sum of three terms:

$$H = H_0 + H_1 + H_2 \tag{15}$$

where H_0, H_1, and H_2 contain the two-spin operators affected by neither, one, and both pulses, respectively:

$$H_0 = \sum_{i\neq k}\sum_{j\neq l}\omega_{C_iN_j}2C_{iz}N_{jz} + \sum_{i<j\neq k}\pi J_{C_iC_j}2C_{iz}C_{jz} \tag{16a}$$

$$H_1 = \sum_{i\neq l}\omega_{C_kN_i}2C_{kz}N_{iz} + \sum_{i\neq k}\omega_{C_iN_l}2C_{iz}N_{lz} + \sum_{i\neq k}\pi J_{C_kC_i}2C_{kz}C_{iz} \tag{16b}$$

$$H_2 = \omega_{C_kN_l}2C_{kz}N_{lz} \tag{16c}$$

The sign of H_1 is inverted by the selective ^{13}C and ^{15}N π pulses, which leads to the refocusing of those interactions during the

FSR pulse sequence. H_0 and H_2 are unaffected by the π pulses, and eq 14 can be simplified to:

$$U(\tau) = \exp\{-iH_0\tau\}\exp\{-iH_2\tau\}\exp\{-i\pi C_{kx}\}\exp\{-i\pi N_{lx}\}$$
$$(17)$$

Furthermore, in the FSR experiment we are only interested in the dipolar dephasing of the transverse magnetization on the ^{13}C spin, C_k, irradiated by the ^{13}C selective pulse, and therefore the initial density matrix is:

$$\rho(\tau_0) = p_k C_{kx} \qquad (18)$$

Since in eq 17 the exponential operators containing H_0, C_{kx}, and N_{lx} commute with the initial density matrix, they have no effect on the time evolution (cf. eq 10) and can be neglected. The resulting propagator for the complete FSR pulse sequence is given by:

$$U(\tau) = \exp\{-i\omega_{C_kN_l}2C_{kz}N_{lz}\} \qquad (19)$$

Therefore, spin C_k evolves only under the dipolar coupling to the selected N_l spin in the multispin system, while the remaining ^{13}C$-^{15}$N dipolar couplings and ^{13}C$-^{13}$C scalar couplings, which would complicate the evolution, are suppressed. The ^{13}C spin$-$echo intensity averaged over the crystallite ensemble is equivalent to that expected for an isolated spin pair under conventional REDOR:[32]

$$S(\tau) = \langle \tilde{p}_k \cos(\omega_{C_kN_l}\tau)\rangle \qquad (20)$$

Experimentally, the frequency selective ^{13}C and ^{15}N pulses do not correspond to instantaneous π rotations, and in our implementation selective excitation of resonances is achieved with weak Gaussian-shaped pulses[67] (e.g., $\sim\pm500$ Hz ^{15}N excitation bandwidth requires a 4 ms pulse). Nevertheless, in practice we find that the selective pulses act in nearly ideal fashion; the effects due to their application appear to be relatively minor and are compensated by recording reference experiments. We also note here that it is *essential* that rotor synchronization is maintained throughout the entire experiment, since for efficient refocusing of the dipolar interactions the phase of the REDOR sequence[25,68] must remain unchanged. We used a standard spinning frequency controller (see Experimental Section), and the resulting ±5 Hz stability in the MAS rate was adequate for maintaining the required rotor synchronization.

Results and Discussion

Selective Recoupling in [U-^{13}C,^{15}N]Asparagine. Asparagine (Figure 2a) represents a favorable model system for demonstrating frequency selective ^{13}C$-^{15}$N recoupling experiments in uniformly ^{13}C,^{15}N-labeled compounds. The difference in C$^\alpha$ and C$^\beta$ isotropic chemical shifts is ~16 ppm, and the N$'$ and N$^{\delta2}$ resonances are separated by ~75 ppm (Figure 2b and 2c), which enables straightforward frequency selective irradiation of ^{13}C$-$^{15}N spin pairs. Furthermore, the four ^{13}C$-^{15}$N dipolar couplings to be measured (Figure 2a) cover a relatively wide range of internuclear distances ($\sim1.5-4$ Å).

Prior to quantitative C$-$N distance determination we qualitatively investigate the selective recoupling of C$^\beta-$N$'$ and C$^\beta-$N$^{\delta2}$ interactions using the FSR pulse sequence. The C$^\beta$ resonance is selectively irradiated with a 1.0 ms Gaussian pulse, and ^{15}N

(67) Freeman, R. *Spin Choreography: Basic Steps in High-Resolution NMR*; Spektrum: Oxford, 1997.

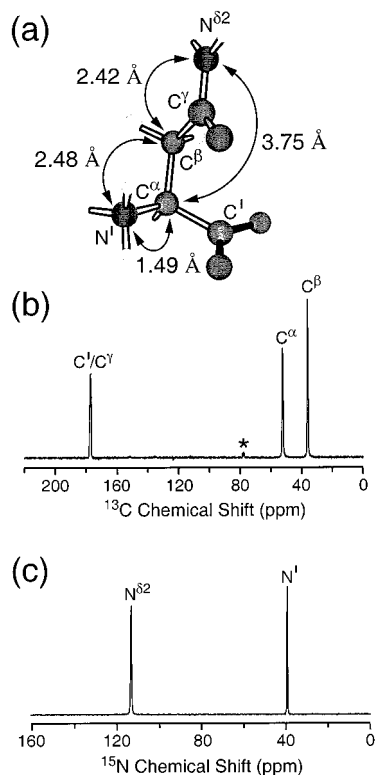(68) Gullion, T.; Conradi, M. S. *J. Magn. Reson.* **1990**, *86*, 39−45.

Figure 2. (a) Neutron diffraction structure of asparagine.[69] The internuclear distances of interest in this work are indicated. ^{13}C (b) and ^{15}N (c) MAS spectra of [U-^{13}C,^{15}N]asparagine recorded at $\omega_r/2\pi = 12.5$ kHz. Rotational sidebands are denoted by an asterisk.

Gaussian pulses are applied at different frequencies in the ^{15}N spectrum. ^{15}N REDOR π pulses are approximately centered between the N$'$ and N$^{\delta2}$ resonances ($\delta \approx 75$ ppm in Figure 2c), so that the effective field during REDOR is identical for both ^{15}N, and the dipolar evolution time (see Figure 1) is set to $\tau = 8.0$ ms. Figure 3 demonstrates the selective recoupling of C$^\beta-$N$'$ and C$^\beta-$N$^{\delta2}$ interactions using a frequency selective spin$-$echo generated by the simultaneous ^{13}C and ^{15}N selective pulses; the C$^\beta$ signal is dephased only by the ^{15}N nuclei on-resonance with the Gaussian pulse, while the couplings to off-resonance ^{15}N are refocused. The selectivity of the FSR experiment can be tuned by adjusting the duration of the ^{15}N Gaussian pulse, where the recoupling conditions become increasingly narrow for long, weak pulses. The recoupling bandwidths obtained with $1-10$ ms pulses are in the ±2000 to ±200 Hz range.

Having demonstrated the feasibility of pairwise recoupling of selected heteronuclear interactions in a multiple-spin system, we apply the FSR experiment to the quantitative measurement of several internuclear distances in [U-^{13}C,^{15}N]asparagine. In Figure 4a and 4b we determine the C$^\beta-$N$'$ and C$^\beta-$N$^{\delta2}$ distances, respectively, where a 1.0 ms ^{13}C selective pulse is applied to the C$^\beta$ resonance, a 1.0 ms ^{15}N selective pulse is applied on-resonance with the ^{15}N to be recoupled, and the dipolar evolution time, τ, is incremented. The simulation of experimental data to the two-spin model (see Experimental Section for details) results in best-fit C$^\beta-$N$'$ and C$^\beta-$N$^{\delta2}$ distances of 2.49 ± 0.02 and 2.44 ± 0.02 Å, respectively; these distances are in good agreement with the neutron diffraction values of 2.48 Å for C$^\beta-$N$'$ and 2.42 Å for C$^\beta-$N$^{\delta2}$.[69]

For comparison with the individual distance measurements, Figure 4c shows the dipolar dephasing in a coupled pseudo-three-spin (N$^{\delta2}-$C$^\beta-$N$'$) system, where simultaneous recoupling of both ^{13}C$-^{15}$N interactions significantly alters the evolution relative to the "spin-pair" cases. The data were simulated using
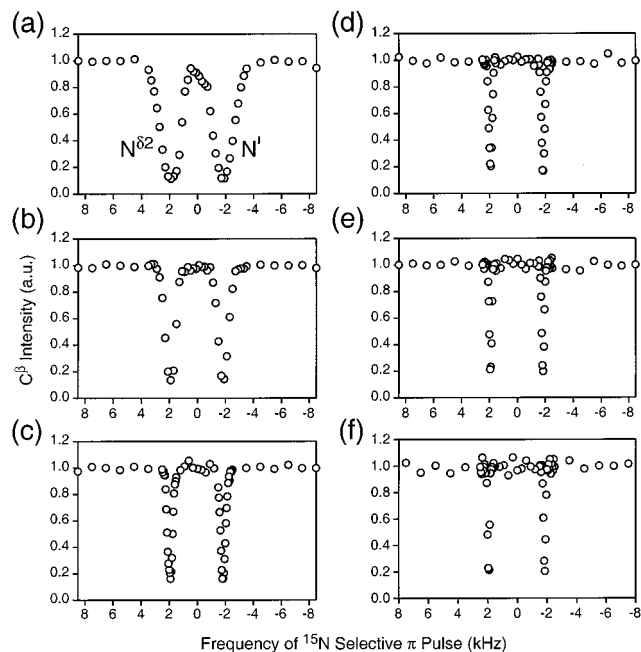
Figure 3. Selective recoupling of $C^\beta-N'$ and $C^\beta-N^{\delta2}$ dipolar interactions in [U-^{13}C,^{15}N]asparagine. The pulse sequence in Figure 1 was used with the total dipolar evolution time, $\tau = 8.0$ ms. Experiments were performed at $\omega_r/2\pi = 10.0$ kHz $\pm$ 5 Hz with a 1.0 ms Gaussian pulse applied to the C^β resonance. We show the results of "frequency sweep" experiments for ^{15}N Gaussian pulses of: (a) 1.0, (b) 2.0, (c) 4.0, (d) 6.0, (e) 8.0, and (f) 10.0 ms. Each experimental point (○) is the ratio of the intensity of the C^β resonance in the presence and absence of the ^{15}N selective pulse. The ^{15}N selective pulse bandwidths, outside of which negligible recoupling takes place, were found to be approximately: (a) $\pm$2000, (b) 1000, (c) 500, (d) 300, (e) 250, and (f) 200 Hz.

the $C^\beta-N'$ and $C^\beta-N^{\delta2}$ couplings determined from FSR experiments (Figure 4a and 4b) with the relative orientation, $\theta_{12} = 123°$, obtained from the neutron diffraction structure,[69] and the agreement between experiment and simulation is good. In this favorable case of two ^{13}C$-^{15}$N couplings of approximately equal magnitude, we can obtain information about both couplings from the nonselective experiment. However, as noted previously, in general the accurate extraction of weak dipolar couplings from dipolar dephasing data in multiple-spin systems of unknown topology is very difficult.[39]

In Figure 5 we show the measurement of $C^\alpha-N'$ and $C^\alpha-N^{\delta2}$ distances in [U-^{13}C,^{15}N]asparagine. It is clear that the rapid dipolar oscillation due to the one-bond $C^\alpha-N'$ coupling is suppressed when the ^{15}N selective pulse is applied off-resonance with N', and selective dephasing of the C^α signal by $N^{\delta2}$ can be accomplished (Figure 5a). We note that for experiments where one-bond ^{13}C$-^{15}$N couplings are refocused the reference and dephasing curves for evolution times greater than ∼10–12 ms can appear somewhat "noisy" relative to experiments involving the refocusing of weaker (e.g., two-bond) couplings. This may be the result of short-term fluctuations in the spinning frequency, the effects of which are expected to be most pronounced at long evolution times when attempting to refocus strong couplings. (In such cases we found that averaging several experiments acquired at different times significantly reduces the scatter in the data.) The experimental data were simulated (Figure 5b and 5c) and the resulting distances are 1.50 $\pm$ 0.02 Å for $C^\alpha-N'$ and 3.58 $\pm$ 0.20 Å for $C^\alpha-N^{\delta2}$. These compare
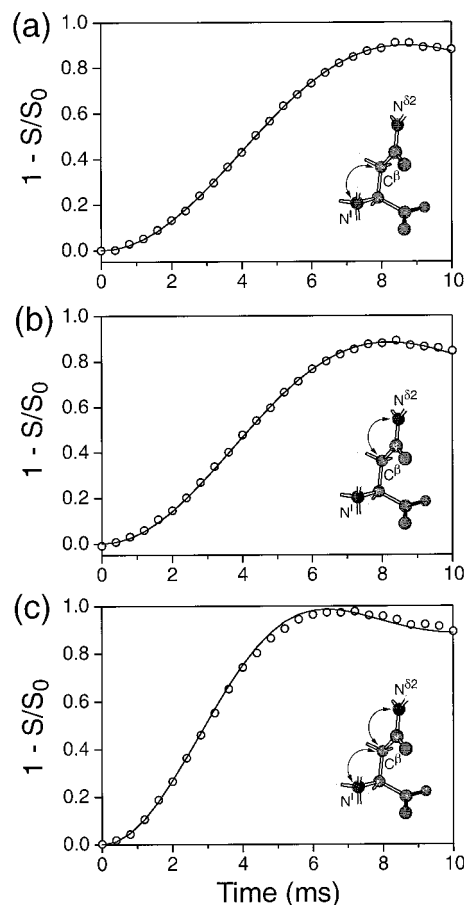
(69) Verbist, J. J.; Lehmann, M. S.; Koetzle, T. F.; Hamilton, W. C. *Acta Crystallogr.* **1972**, *B28*, 3006.

Figure 4. Internuclear distance measurements for C^β in [U-^{13}C,^{15}N]-asparagine and dipolar evolution in the coupled pseudo-three-spin system $N^{\delta2}-C^\beta-N'$. Pairwise frequency selective recoupling of $C^\beta-N'$ (a) and $C^\beta-N^{\delta2}$ (b) interactions. Experiments were performed at $\omega_r/2\pi = 10.0$ kHz $\pm$ 5 Hz, and eight scans were averaged for each time point. A 1.0 ms Gaussian pulse was applied to the C^β resonance, and a 1.0 ms Gaussian pulse was applied on resonance with N' (a) or $N^{\delta2}$ (b). The simulations (—) in (a) and (b) are least-squares fits of the experimental data (○) to the analytical expression describing the dipolar evolution in an isolated heteronuclear spin pair under conventional REDOR, where finite pulse effects have been taken into account. The best-fit values for the dipolar coupling constants are $b_{CN}(C^\beta-N') = 198 \pm 3$ Hz and $b_{CN}(C^\beta-N^{\delta2}) = 210 \pm 3$ Hz, corresponding to $C^\beta-N'$ and $C^\beta-N^{\delta2}$ distances of 2.49 $\pm$ 0.02 and 2.44 $\pm$ 0.02 Å, respectively (cf. Table 1). In (c) we show experimental data (○) and simulation (—) for the *J*-decoupled REDOR experiment,[53] in which $C^\beta-N'$ and $C^\beta-N^{\delta2}$ interactions are simultaneously recoupled and the dipolar dephasing of the C^β spin depends on both ^{13}C$-^{15}$N couplings and their relative orientation (see text for details). The input parameters for the simulation are the $C^\beta-N'$ and $C^\beta-N^{\delta2}$ dipolar couplings (determined to be 198 and 210 Hz from the FSR experiments in (a) and (b)) and the projection angle between the $C^\beta-N'$ and $C^\beta-N^{\delta2}$ dipole vectors (determined to be $\theta_{12} = 123°$ from the asparagine neutron diffraction structure[69]).

well with the respective neutron diffraction distances of 1.49 and 3.75 Å.[69] A summary of all distance measurements in [U-^{13}C,^{15}N]asparagine is provided in Table 1.

Internuclear Distance Measurements in U-^{13}C,^{15}N-Labeled Peptides. In the following we present accurate ^{13}C$-^{15}$N distance measurements in model peptides, [U-^{13}C,^{15}N]*N*-acetyl-L-Val-L-Leu (VL) and *N*-formyl-[U-^{13}C,^{15}N]L-Met-L-Leu-L-Phe (MLF). Frequency selective recoupling in these peptides is more challenging compared to that in asparagine, since the amide ^{15}N resonances have very similar frequencies. However, we found that 6–10 ms ^{15}N Gaussian pulses, having ∼$\pm$300 to $\pm$200
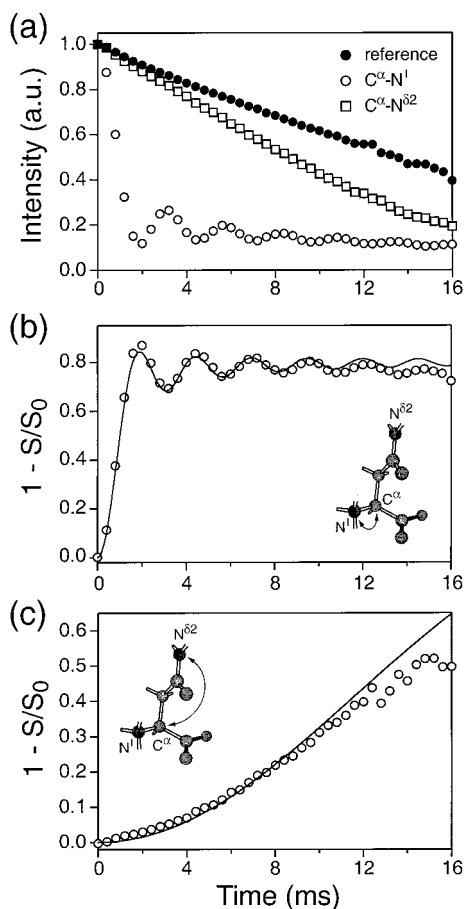
Figure 5. Internuclear distance measurements for C^α in [U-^{13}C,^{15}N]-asparagine. (a) Reference (S_0) curve (●) and dipolar dephasing (S) curves for C^α−N′ (○) and C^α−$N^{\delta 2}$ (□) couplings. Experimental $\Delta S/S_0$ curves (○) and analytical simulations (—) for C^α−N′ (b) and C^α−$N^{\delta 2}$ (c) couplings. The best-fit values for the dipolar coupling constants are $b_{CN}(C^\alpha$−N′$) = 907 \pm 35$ Hz and $b_{CN}(C^\alpha$−$N^{\delta 2}) = 67 \pm 8$ Hz, corresponding to C^α−N′ and C^α−$N^{\delta 2}$ distances of 1.50 ± 0.02 and 3.58 ± 0.20 Å, respectively (cf. Table 1). Spectra were recorded at $\omega_r/2\pi = 10.0$ kHz ± 5 Hz, and 6 experiments (eight scans per experiment) were averaged for each time point. A 1.0 ms Gaussian pulse was applied to the C^α resonance, and a 1.0 ms Gaussian pulse was applied on resonance with N′ (b) and $N^{\delta 2}$ (c).

Table 1. Internuclear Distances in [U-^{13}C,^{15}N]Asparagine

		r_{C-N} (Å)	
atoms[a]		NMR[b]	neutron[c]
N′	C^α	1.50 ± 0.02	1.49
	C^β	2.49 ± 0.02	2.48
$N^{\delta 2}$	C^α	3.58 ± 0.20	3.75
	C^β	2.44 ± 0.02	2.42

[a] Nomenclature given in Figure 2a. [b] NMR distances (with uncertainties at 95% confidence level) were determined using frequency selective REDOR as described in the text. [c] Verbist, J. J.; Lehmann, M. S.; Koetzle, T. F.; Hamilton, W. C. *Acta Crystallogr.* **1972**, *B28*, 3006.

Hz bandwidths (cf. Figure 3), were sufficient to selectively recouple the individual amide ^{15}N in VL and MLF.

Figure 6 shows the X-ray structure of *N*-acetyl-L-Val-L-Leu[62] as well as one-dimensional ^{13}C and ^{15}N MAS spectra of the U-^{13}C,^{15}N-labeled peptide. The ^{13}C and ^{15}N chemical shift assignments were obtained from two-dimensional ^{13}C−^{13}C and ^{13}C−^{15}N correlation experiments (see Supporting Information). The ^{13}C−^{13}C correlation spectra do not provide unambiguous assignments for the Val and Leu methyl resonances. The assignment of the Leu(C^δ) resonances remains ambiguous since
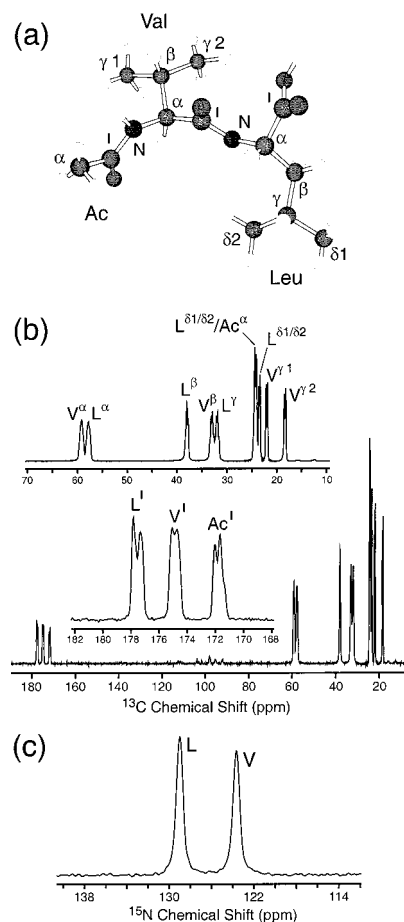

Figure 6. X-ray structure of *N*-acetyl-L-Val-L-Leu[62] (a) and ^{13}C (b) and ^{15}N (c) MAS spectra of [U-^{13}C,^{15}N]*N*-acetyl-L-Val-L-Leu recorded at $\omega_r/2\pi = 10.0$ kHz. Most ^{13}C resonances exhibit resolved splittings due to $\sim$30−60 Hz ^{13}C−^{13}C J couplings. ^{13}C and ^{15}N chemical shift assignments were obtained from two-dimensional ^{13}C−^{13}C and ^{13}C−^{15}N correlation spectra (see Supporting Information). Val($C^{\gamma 1}$) and Val-($C^{\gamma 2}$) resonances were assigned on the basis of the FSR experiments presented in this work. Assignment of Leu($C^{\delta 1}$) and Leu($C^{\delta 2}$) resonances remains ambiguous, since distance measurements involving those nuclei were not performed here.

we did not attempt to perform ^{13}C−^{15}N distance measurements involving those ^{13}C. However, using the FSR experiments for both Val(C^γ) we were able to assign the downfield resonance (denoted $C^{\gamma 1}$) to the CH$_3$ approximately *syn* to Val(N) and the upfield resonance (denoted $C^{\gamma 2}$) to the CH$_3$ approximately *anti* to Val(N) (cf. Figure 6a).

Representative FSR experiments in [U-^{13}C,^{15}N]*N*-acetyl-L-Val-L-Leu are presented in Figure 7, and all distances measured in the peptide are summarized in Table 2. The frequency selective experiments enable the measurement of internuclear distances, which provide indispensable information about the three-dimensional structure of the peptide, but are not easily accessible via nonselective methods. For example, Val(C^β) can be recoupled to Val(N) and Leu(N) in separate experiments. While the two-bond Val(C^β)-Val(N) dipolar coupling (Figure 7a), which would dominate the nonselective experiment, provides no useful structural data, the Val(C^β)-Leu(N) coupling (Figure 7b) provides valuable information about the backbone torsion angle ψ_1. Since [U-^{13}C,^{15}N]VL was not diluted in the natural abundance compound, the distances reported are limited to the side chain-to-backbone distances in the 2.5−3.5 Å range, for which the dipolar dephasing depends primarily on a single intramolecular coupling (see Supporting Information). (Accurate
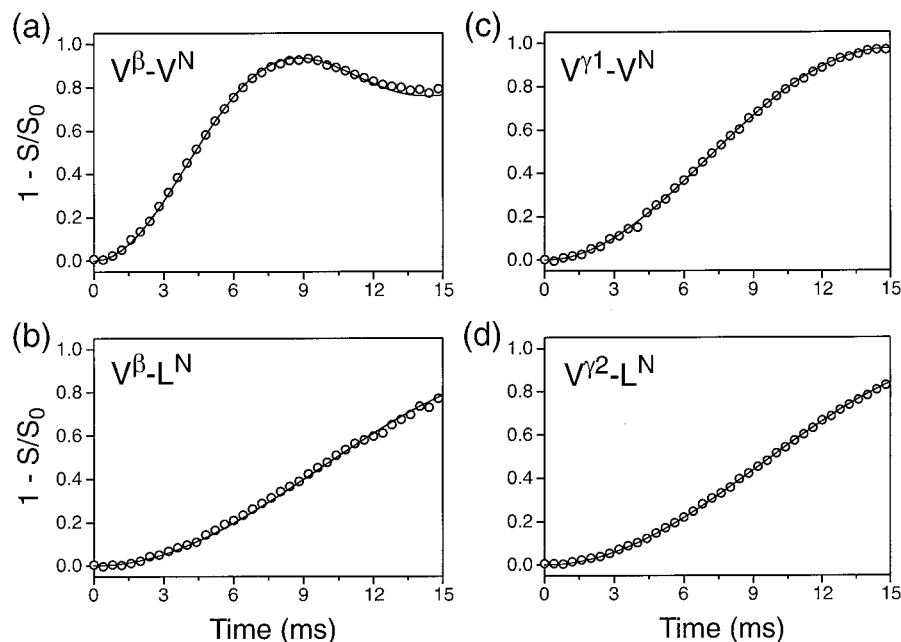
Figure 7. Representative internuclear distance measurements in [U-^{13}C,^{15}N]*N*-acetyl-L-Val-L-Leu. Experimental $\Delta S/S_0$ curves (○) and analytical simulations (—) are shown for the selective pairwise recoupling of (a) Val(C$^\beta$)-Val(N), (b) Val(C$^\beta$)-Leu(N), (c) Val(C$^{\gamma 1}$)-Val(N), and (d) Val(C$^{\gamma 2}$)-Leu(N). The internuclear distances measured in [U-^{13}C,^{15}N]*N*-acetyl-L-Val-L-Leu are summarized in Table 2. Experiments were performed at $\omega_r/2\pi$ = 10.0 kHz ± 5 Hz, and 32 scans were averaged for each time point. The ^{13}C Gaussian pulse was 3.0 ms for experiments involving Val(C$^{\gamma 1}$) and Val(C$^{\gamma 2}$), and 5.0 ms for Val(C$^\beta$), Leu(C$^\beta$) and Leu(C$^\gamma$). The (i) Val(C$^{\gamma 1}$)/Val(C$^{\gamma 2}$) and (ii) Val(C$^\beta$)/Leu(C$^\gamma$) distance measurements were performed simultaneously since the chemical shifts are similar for these nuclei, and Val(C$^{\gamma 1}$)-Val(C$^{\gamma 2}$) and Val(C$^\beta$)-Leu(C$^\gamma$) ^{13}C−^{13}C J couplings are negligible relative to the ^{13}C−^{15}N dipolar couplings of interest. The ^{15}N Gaussian pulse was 10.0 ms, applied on resonance with the Val(N) or Leu(N) resonances.

Table 2. Internuclear Distances in [U-^{13}C,^{15}N]*N*-acetyl-L-Val-L-Leu

		r_{C-N} (Å)	
atoms[a]		NMR[b]	X-ray[c]
Val(N)	Val(C$^\beta$)	2.50 ± 0.02	2.48
	Val(C$^{\gamma 1}$)	3.01 ± 0.02	2.97
	Val(C$^{\gamma 2}$)	3.58 ± 0.08[d]	3.81
Leu(N)	Val(C$^\beta$)	3.35 ± 0.06	3.46
	Val(C$^{\gamma 2}$)	3.31 ± 0.03	3.40
	Leu(C$^\beta$)	2.51 ± 0.02	2.49
	Leu(C$^\gamma$)	3.28 ± 0.06	3.29

[a] Nomenclature given in Figure 6a. [b] NMR distances (with uncertainties at 95% confidence level) were determined using frequency selective REDOR as described in the text. [c] Courtesy of W. Davis (MIT). All distances agree to 0.02 Å or better with those determined in ref 62. [d] The magnitude of intermolecular Val(C$^{\gamma 2}$)-Val(N) couplings (see Supporting Information) is non-negligible relative to the intramolecular Val(C$^{\gamma 2}$)-Val(N) coupling.

measurements of longer distances are demonstrated below for MLF.) Overall the experimental data are reproduced well by the analytical two-spin model (cf. eq 1), and most measured distances agree closely (within ~0.1 Å) with those determined by X-ray crystallography (see Table 2).

The X-ray structure of *N*-formyl-L-Met-L-Leu-L-Phe-OMe,[63] which is closely related to the MLF peptide investigated in this work, is shown in Figure 8a. Figure 8b and 8c show one-dimensional ^{13}C and ^{15}N MAS spectra, respectively, of *N*-formyl-[U-^{13}C,^{15}N]L-Met-L-Leu-L-Phe. The ^{13}C and ^{15}N chemical shift assignments were reported previously in ref 70. The FSR experiments presented here were used to assign the Leu methyl resonances. ^{13}C−^{15}N distance measurements were not performed for the downfield resonance (denoted C$^{\delta 1}$) due to spectral overlap with Leu(C$^\gamma$) (the Leu(C$^\gamma$)-Leu(C$^\delta$) J coupling is ~30 Hz). The MLF-OMe X-ray structure[63] indicates that only one

Leu(C$^\delta$) is in close proximity to Leu(N). For the upfield resonance (denoted C$^{\delta 2}$) the dipolar coupling to Leu(N) was found to be relatively strong; assuming similar structures for MLF and MLF-OMe, we have tentatively assigned the upfield resonance to the CH$_3$ closer to Leu(N) (cf. Figure 8a).

Representative FSR experiments in *N*-formyl-[U-^{13}C,^{15}N]L-Met-L-Leu-L-Phe (undiluted in natural abundance MLF) are shown in Figure 9. For example, the Met(C$^\beta$)-Phe(N) dipolar coupling can be observed in the presence of the stronger Met-(C$^\beta$)-Met(N) and Met(C$^\beta$)-Leu(N) couplings (Figure 9d); the measured Met(C$^\beta$)-Phe(N) distance (short relative to that expected for an extended β-sheet-type structure) identifies the turn in the MLF backbone (see Figure 10). Table 3 provides the summary of all internuclear distances determined in [U-^{13}C,^{15}N]MLF diluted to ~10% in the natural abundance peptide. (Figure 10 shows the X-ray structure of *N*-formyl-L-Met-L-Leu-L-Phe-OMe with several structure-constraining distances determined in MLF superimposed.) Accurate determinations of internuclear distances up to ~6 Å could be performed, and of the total 16 measured distances, 14 are in the 3−6 Å range and provide valuable structural constraints. Most measured distances in MLF are in relatively good agreement with the corresponding distances in the X-ray structure of MLF-OMe.[63] This indicates that, while the three-dimensional structures of MLF and MLF-OMe are not identical, there appears to be a high degree of similarity between them.

Effect of ^{1}H Decoupling on REDOR Experiments. Although insufficient proton decoupling during REDOR does not prohibit the measurement of relatively accurate ^{13}C−^{15}N dipolar couplings,[71] the quality of the experimental data depends on the efficient attenuation of the dipolar contacts between the low-γ nuclei and protons. We find that for REDOR sequences

(70) Hong, M.; Griffin, R. G. *J. Am. Chem. Soc.* **1998**, *120*, 7113−7114.

(71) Mehta, A. K.; Hirsh, D. J.; Oyler, N.; Drobny, G. P.; Schaefer, J. *J. Magn. Reson.* **2000**, *145*, 156−158.
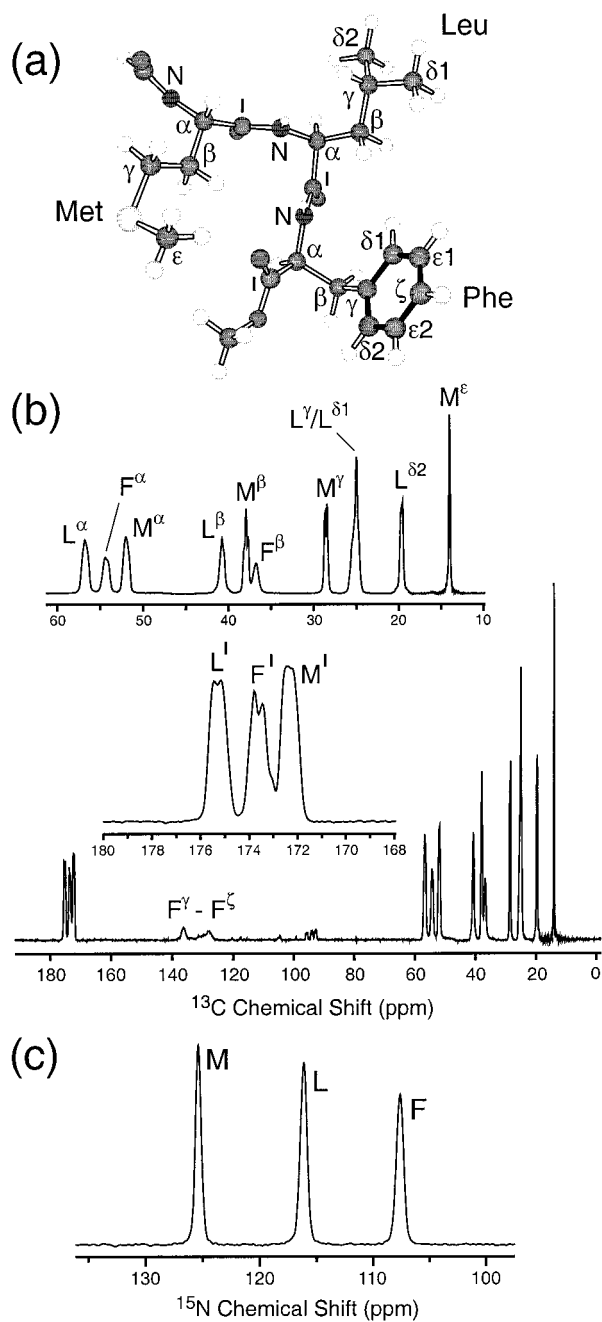
Figure 8. X-ray structure of *N*-formyl-L-Met-L-Leu-L-Phe-OMe[63] (a) and ¹³C (b) and ¹⁵N (c) MAS spectra of *N*-formyl-[U-¹³C,¹⁵N]L-Met-L-Leu-L-Phe recorded at $\omega_r/2\pi = 10.0$ kHz. ¹³C and ¹⁵N chemical shift assignments have been reported previously,[70] and the assignment of Leu(C$^{\delta 1}$) and Leu(C$^{\delta 2}$) resonances is based on FSR experiments presented in this work.

Table 3. Internuclear Distances in *N*-Formyl-[U-¹³C,¹⁵N]L-Met-L-Leu-L-Phe[a]

atoms[b]		r_{C-N} (Å)	
		NMR[c]	X-ray[d]
Met(N)	Met(C$^{\beta}$)	2.52 ± 0.02	2.50
	Met(C$^{\gamma}$)	3.20 ± 0.03	3.04
	Met(C$^{\epsilon}$)	5.4 ± 0.3	5.71
	Leu(C$^{\beta}$)	5.7 ± 0.7	6.03
	Leu(C$^{\delta 2}$)	5.5 ± 0.3	6.28
Leu(N)	Met(C$^{\beta}$)	3.12 ± 0.03	3.20
	Met(C$^{\gamma}$)	4.17 ± 0.10	4.56
	Met(C$^{\epsilon}$)	5.5 ± 0.3	5.93
	Leu(C$^{\beta}$)	2.46 ± 0.02	2.50
	Leu(C$^{\delta 2}$)	3.64 ± 0.09	3.63
Phe(N)	Met(C')	3.4 ± 0.2	3.41
	Met(C$^{\beta}$)	4.12 ± 0.15	4.06
	Met(C$^{\gamma}$)	4.8 ± 0.2	5.43
	Met(C$^{\epsilon}$)	5.2 ± 0.3	5.62
	Leu(C$^{\beta}$)	3.24 ± 0.12	3.12
	Leu(C$^{\delta 2}$)	5.4 ± 0.3	5.38

^{a} *N*-formyl-[U-¹³C,¹⁵N]L-Met-L-Leu-L-Phe was diluted to ∼10% in the natural abundance peptide to attenuate intermolecular ¹³C−¹⁵N contacts. ^{b} Nomenclature given in Figure 8a. ^{c} NMR distances (with uncertainties at 95% confidence level) were determined using frequency selective REDOR as described in the text. ^{d} For comparison with the NMR results, distances are given for the methyl ester analogue, *N*-formyl-L-Met-L-Leu-L-Phe-OMe (Gavuzzo, E.; Mazza, F.; Pochetti, G.; Scatturin, A. *Int. J. Pept. Protein Res.* **1989**, *34*, 409).

decoupling was used, and we observe a significant improvement in the ¹³C spin−echo intensity with TPPM decoupling (Figure 11a). This effect is of practical importance for systems yielding spectra with low signal-to-noise ratios. However, inefficient ¹H decoupling during the free-evolution periods is effectively compensated by the $\Delta S/S_0$ analysis, as nearly identical $\Delta S/S_0$ curves are obtained for both decoupling schemes (Figure 11b).

The effects of insufficient ¹H decoupling during the ¹⁵N rf pulses cannot be compensated with reference experiments. In Figure 12 we investigate these effects in spin systems with different ¹⁵N−¹H dipolar couplings by acquiring a series of dipolar dephasing curves in the presence of CW decoupling held constant at ∼85 kHz and ¹⁵N rf fields of ∼25, 35 and 50 kHz. For [1-¹³C,¹⁵N]glycine (Figure 12a and 12b), where the strong ¹⁵N−¹H interactions are attenuated by the rapid hopping of the NH₃⁺ group under the experimental conditions employed here,[75] the effects of ¹⁵N−¹H recoupling due to the insufficient mismatch of ¹H and ¹⁵N rf fields[72−74] appear to be minimal (Figure 12a), and the $\Delta S/S_0$ curves recorded for different ¹⁵N fields are nearly identical (Figure 12b). The situation is quite different in the case of the relatively rigid amide group in [acetyl-1,2-¹³C,¹⁵N]*N*-acetylvaline, for which the ¹⁵N−¹H coupling is strong (∼10 kHz). Here, both reference and dipolar dephasing curves for the (acetyl-CH₃)−N′ coupling (Figure 12c) show significant deviations from ideal behavior for $\omega_{rf}(^1H):\omega_{rf}(^{15}N)$ less than 3:1.[72−74] The resulting $\Delta S/S_0$ curves (Figure 12d) display a significant amplitude scaling (∼15%) as $\omega_{rf}(^1H):\omega_{rf}(^{15}N)$ changes from ∼3.5 to 1.5. However, regardless of the rf field mismatch, the $\Delta S/S_0$ curves in NAV could be simulated (not shown) with approximately the same dipolar coupling constant ($b_{CN} = 211 ± 2$ Hz), but different amplitude scaling factors.

of the type shown in Figure 1 (where all recoupling π pulses are applied to the nonobserved spins) reference experiments can be used to compensate for insufficient proton decoupling during the delays between the pulses; however, insufficient decoupling during the π pulses can result in a significant scaling of the dipolar dephasing amplitude.

Figure 11 shows a comparison of ¹H decoupling schemes during the dipolar evolution period of FSR experiments in [U-¹³C,¹⁵N]asparagine. The ¹⁵N rf field was ∼28 kHz, and the ¹H decoupling field during the ¹⁵N π pulses was 125 kHz CW in all experiments, ensuring a sufficiently high $\omega_{rf}(^1H):\omega_{rf}(^{15}N)$ mismatch.[72−74] During the delays between the pulses, 120 kHz continuous wave (CW) or two-pulse phase modulation (TPPM)[59]

(72) Ishii, Y.; Ashida, J.; Terao, T. *Chem. Phys. Lett.* **1995**, *246*, 439−445.

(73) Bennett, A. E. Ph.D. Thesis, Massachusetts Institute of Technology, 1995.

(74) Bennett, A. E.; Rienstra, C. M.; Griffiths, J. M.; Zhen, W.; Lansbury, P. T.; Griffin, R. G. *J. Chem. Phys.* **1998**, *108*, 9463−9479.

(75) Long, J. R.; Sun, B. Q.; Bowen, A.; Griffin, R. G. *J. Am. Chem. Soc.* **1994**, *116*, 11950−11956.
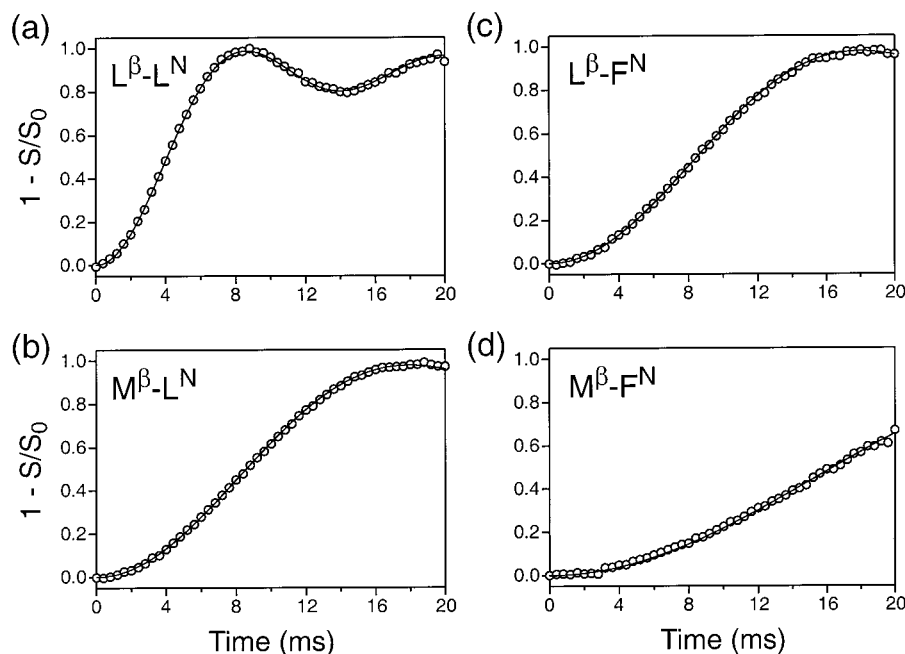
Figure 9. Representative internuclear distance measurements in *N*-formyl-[U-^{13}C,^{15}N]L-Met-L-Leu-L-Phe. Experimental $\Delta S/S_0$ curves (○) and analytical simulations (—) are shown for the selective pairwise recoupling of (a) Leu(C$^\beta$)-Leu(N), (b) Met(C$^\beta$)-Leu(N), (c) Leu(C$^\beta$)-Phe(N), and (d) Met-(C$^\beta$)-Phe(N). The experiments shown have been performed on [U-^{13}C,^{15}N]MLF undiluted in natural abundance material, but are not appreciably affected by intermolecular couplings (see Supporting Information). Experiments were performed at $\omega_r/2\pi = 10.0$ kHz $\pm$ 5 Hz, and 32 scans were averaged for each time point. The ^{13}C Gaussian pulse was 2.0 ms for experiments involving Met(C$^\beta$) and Leu(C$^\beta$), and 4.0 ms for Met(C$^\gamma$) and Leu(C$^{\delta 2}$). The Met(C$^\beta$)/Leu(C$^\beta$) distance measurements were performed simultaneously. The ^{15}N Gaussian pulse was 10.0 ms, applied on resonance with Met(N), Leu(N) or Phe(N). The summary of all distance measurements in *N*-formyl-[U-^{13}C,^{15}N]L-Met-L-Leu-L-Phe is given in Table 3.
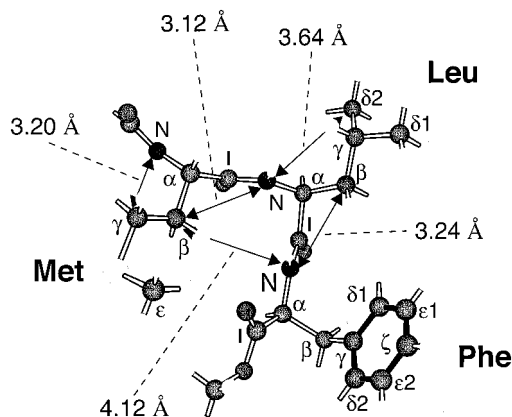

Figure 10. X-ray structure of *N*-formyl-L-Met-L-Leu-L-Phe-OMe with several structure-constraining distances determined in 10% diluted *N*-formyl-[U-^{13}C,^{15}N]L-Met-L-Leu-L-Phe superimposed (cf. Table 3).

As shown by others[71] and suggested by the experiments presented here, in many cases reasonably accurate distances can be obtained using REDOR even in the presence of relatively low-power CW ^{1}H decoupling. However, significant scaling of the dipolar dephasing amplitude may potentially become problematic for weak coupling measurements, where $\Delta S/S_0$ buildup is slow. The efficient attenuation of proton couplings significantly improves the ^{13}C spin–echo intensity and avoids the scaling of the dipolar dephasing amplitude in spin systems with strong ^{15}N–^{1}H couplings. Efficient proton decoupling does not necessarily imply the use of very high-power levels. When only moderate ^{1}H rf fields (e.g., ~80 kHz) are available due to probe limitations, TPPM decoupling during delays between ^{15}N pulses (see Figure 1) effectively restores the spin–echo intensity, and the use of slightly longer ^{15}N π pulses provides a sufficiently high $\omega_{rf}(^1H):\omega_{rf}(^{15}N)$ ratio required to minimize the ^{15}N–^{1}H interactions.
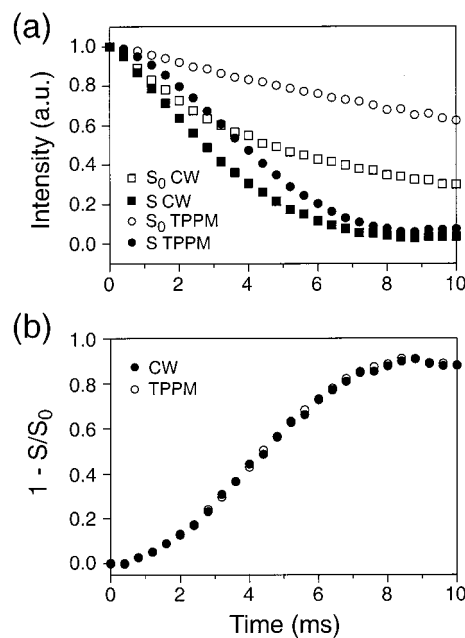

Figure 11. Comparison of ^{1}H decoupling schemes during the dipolar evolution period of FSR experiments in [U-^{13}C,^{15}N]asparagine. Results for the selective recoupling of C$^\beta$–N′ are shown. (Identical results were obtained for C$^\beta$–N$^{\delta 2}$.) Experiments were performed at $\omega_r/2\pi = 10.0$ kHz $\pm$ 5 Hz, and eight scans were averaged for each time point. ^{15}N π pulses were 18 μs, and 1.0 ms Gaussian pulses were applied to C$^\beta$ and N′. For all experiments ^{1}H decoupling was 125 kHz CW during ^{15}N π pulses and 120 kHz TPPM ($\phi = 15°$, $\tau = 4.0$ μs) during the selective irradiation period. (a) Reference (S_0) (□,○) and dipolar dephasing (S) (■,●) experiments recorded in the presence of 120 kHz CW (□,■) and TPPM (○,●) ^{1}H decoupling during the free-evolution periods corresponding to delays between ^{15}N π pulses. (b) $\Delta S/S_0$ curves calculated using data in (a) for CW (●) and TPPM (○) ^{1}H decoupling.
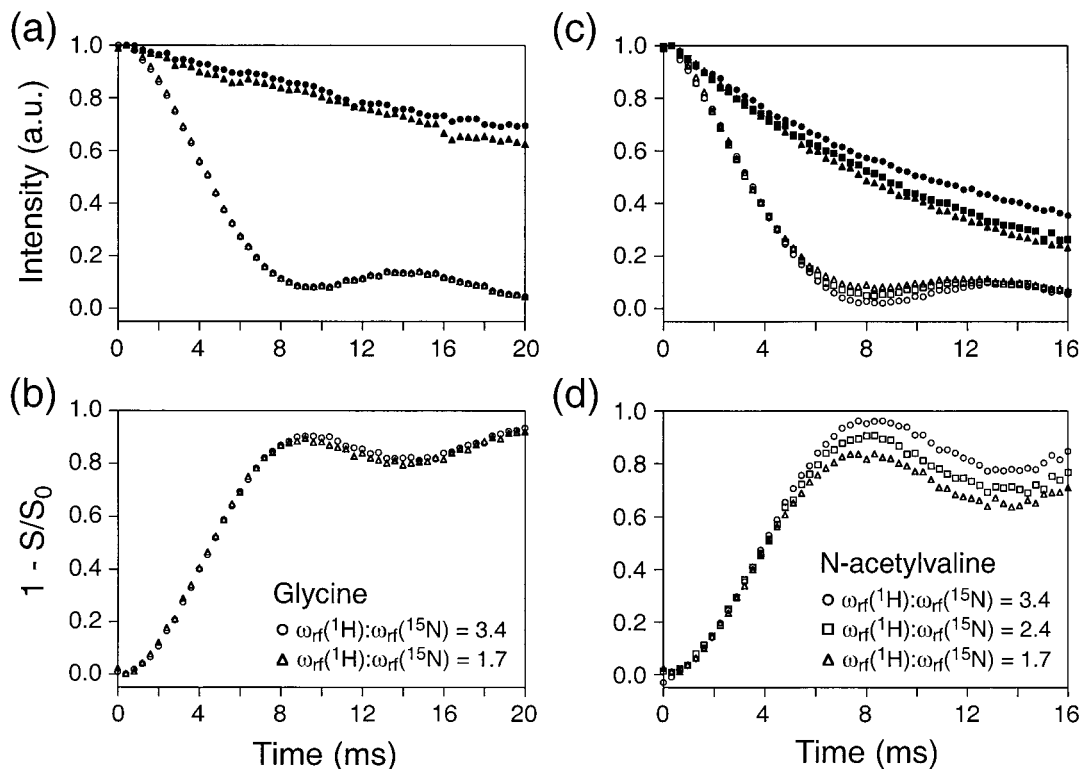
Figure 12. Effect of ^{1}H decoupling during periods corresponding to ^{15}N pulses in spin systems with ^{15}N$-^1$H dipolar couplings of different magnitude. Dipolar recoupling data are presented for [1-^{13}C,^{15}N]glycine (a$-$b), for which the ^{15}N$-^1$H couplings are effectively attenuated by the rapid hopping of the NH$_3^+$ group under the experimental conditions employed in this work,[75] and for [acetyl-1,2-^{13}C,^{15}N]*N*-acetylvaline (NAV) (c$-$d), where the relatively rigid amide group displays a strong ($\sim$10 kHz) ^{15}N$-^1$H dipolar coupling. Experiments were performed at $\omega_r/2\pi = 12.5$ kHz $\pm$ 5 Hz, and 16 scans were averaged for each time point. In (a) and (c) we show S_0 (filled symbols) and S (hollow symbols) curves for the $\sim$200 Hz ^{13}C$-^{15}$N dipolar couplings in both compounds (C$'$$-N'$ in glycine and (acetyl-CH$_3$)$-$N$'$ in NAV). All S_0 experiments were acquired in the presence of ^{15}N π pulses. ^{1}H decoupling was fixed at $\sim$85 kHz CW for all experiments, and the ^{15}N π-pulse lengths were 20 μs ($\bullet$,$\circ$), 14 μs ($\blacksquare$,$\square$), and 10 μs ($\blacktriangle$,$\triangle$), corresponding to ^{15}N rf fields of 25 kHz ($\omega_{rf}(^1$H):$\omega_{rf}(^{15}$N) $\approx$ 3.4), 35.7 kHz ($\omega_{rf}(^1$H):$\omega_{rf}(^{15}$N) $\approx$ 2.4), and 50 kHz ($\omega_{rf}(^1$H):$\omega_{rf}(^{15}$N) $\approx$ 1.7), respectively. The ^{13}C spin$-$echo reference curves acquired with no ^{15}N irradiation (data not shown) were identical within experimental error to the S_0 experiments acquired in the presence of 20 μs ^{15}N π pulses. $\Delta S/S_0$ curves calculated using S_0 and S experiments in (a) and (c) are shown for glycine (b) and NAV (d) for ^{15}N π pulses of 20 μs ($\bigcirc$), 14 μs ($\square$), and 10 μs ($\triangle$). In (a) and (b) the glycine data for 14 μs ^{15}N π pulses have been omitted for clarity.

Effect of ^{15}N CSA on REDOR Experiments. In Figure 13 we present experimental data and numerical simulations showing the effect of the chemical shielding anisotropy (CSA) of the irradiated spins (^{15}N in our case) on REDOR dipolar dephasing curves acquired with several commonly used compensated π-pulse phasing schemes ($xy-4$, $xy-8$, and $xy-16$).[33] [1-^{13}C,^{15}N]-Glycine, with a negligible ^{15}N CSA ($\delta \approx 5$ ppm, $\eta = 0$),[75] is used as a reference, and as expected $\Delta S/S_0$ curves recorded with $xy-4$, $xy-8$, and $xy-16$ (Figure 13a) are nearly identical. The situation is quite different for a larger ^{15}N CSA ($\delta = 106$ ppm, $\eta = 0.27$)[76] in [acetyl-1,2-^{13}C,^{15}N]NAV, where significant effects are observed in the presence of $xy-16$ phase cycling relative to $xy-4$ and $xy-8$ (Figure 13b). The experimental observations are compared to numerical simulations (performed with the SIMPSON simulation software[77]) (Figure 13c). For the "two-spin" (acetyl-CH$_3$)$-$N$'$ system (see Figure 13 caption for details) the $\Delta S/S_0$ curves simulated for the $xy-4$ and $xy-8$ schemes are nearly identical and closely follow the result for finite pulse REDOR in the absence of ^{15}N CSA. However, an amplitude scaling is observed in the $xy-16$ simulation, which reproduces the experimental result shown in Figure 13b. The experiments and simulations presented here suggest that $xy-4$ and $xy-8$ are equally well-compensated for ^{15}N CSA effects.

However, additional simulations (not shown) indicate that for increasing CSA the dephasing curves for all phasing schemes can display some scaling of amplitude and frequency of the oscillation; in general, $xy-4$ simulations appear to most closely approach the ideal dipolar dephasing curve.

The influence of ^{15}N CSA on REDOR dipolar dephasing with several simple phasing schemes ($xx-4$, $x\bar{x}-4$, and $xy-4$) has been discussed previously using Floquet theory.[78] According to average Hamiltonian theory,[64,65] for ^{13}C-observe REDOR with ^{15}N π pulses of finite length phased according to $xy-4$ or extensions thereof (see Figure 1), the ^{15}N CSA is not expected to contribute to the spin dynamics to first-order. In the rf interaction frame the ^{15}N pulses transform only the N_z operator and the first-order effective Hamiltonian for the ^{15}N CSA is analogous to that calculated for the heteronuclear dipolar coupling (cf. eqs 2 and 3):

$$H_{CSA}^{(1)} \propto \mathrm{Im}\{\omega_{CSA}^{(1)}(\Omega_{PR})\}N_z \qquad (21)$$

where $\omega_{CSA}^{(1)}$ describes the transformation of the ^{15}N CSA tensor from its principal axis system to the rotor-fixed frame.[66] Since the experiments are designed to follow the time evolution

(76) Hong, M.; Gross, J. D.; Hu, W.; Griffin, R. G. *J. Magn. Reson.* **1998**, *135*, 169$-$177.

(77) Bak, M.; Rasmussen, J. T.; Nielsen, N. C. *J. Magn. Reson.* **2000**, *147*, 296$-$330.
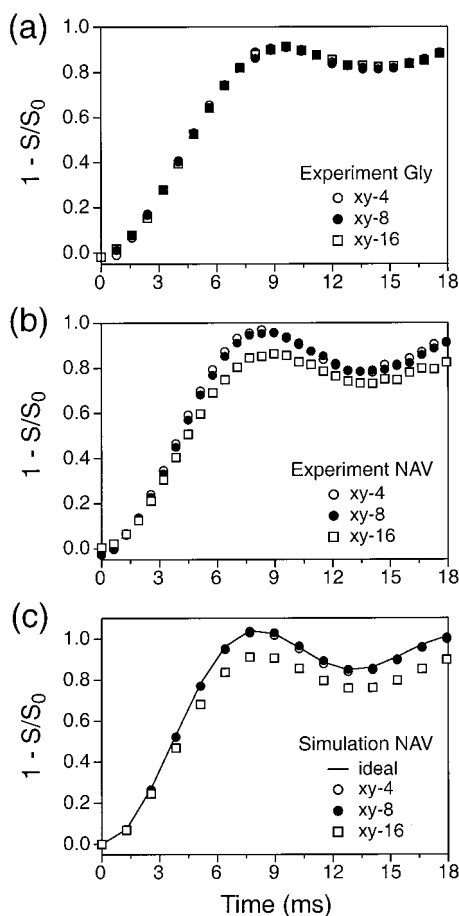
(78) Weintraub, O.; Vega, S. *J. Magn. Reson. A* **1993**, *105*, 245$-$267.

(79) Oas, T. G.; Hartzell, C. J.; Dahlquist, F. W.; Drobny, G. P. *J. Am. Chem. Soc.* **1987**, *109*, 5962$-$5966.

(80) Bax, A. *Two-Dimensional Nuclear Magnetic Resonance in Liquids*; Delft University Press: Dordrecht, 1980.

Figure 13. Effect of ^{15}N chemical shielding anisotropy on ^{13}C-observe REDOR experiments. Three common ^{15}N π-pulse phase cycling schemes[33] (*xy*−4 (○), *xy*−8 (●), and *xy*−16 (□)), designed to compensate for pulse errors and resonance offsets, are compared in (a) and (b). We show REDOR experiments for C′−N′ coupling in [1-^{13}C,^{15}N]glycine (^{15}N CSA: $\delta \approx 5$ ppm, $\eta = 0$)[75] (a) and (acetyl-CH$_3$)−N′ coupling in [acetyl-1,2-^{13}C,^{15}N]*N*-acetylvaline (^{15}N CSA: $\delta = 106$ ppm, $\eta = 0.27$)[76] (b). Spectra were recorded at $\omega_r/2\pi = 12.5$ kHz $\pm$ 5 Hz, and four experiments (16 scans per experiment) were averaged for each time point. (c) Simulated REDOR $\Delta S/S_0$ curves assuming the (acetyl-CH$_3$)−N′ dipolar coupling constant ($b_{CN} = 220$ Hz) obtained from the NAV X-ray structure[62] and finite ^{15}N π pulses for: no ^{15}N CSA ($\delta = \eta = 0$) (—), and ^{15}N CSA parameters of NAV[76] at $B_0 = 11.7$ T ($\delta = 5.37$ kHz, $\eta = 0.27$) with *xy*−4 (○), *xy*−8 (●), and *xy*−16 (□) phase-alternation of ^{15}N π pulses. The spinning frequency of 12.5 kHz was used in the simulations, and the orientation of the amide ^{15}N CSA tensor in the molecular frame given in ref 79 was assumed (σ_{22} perpendicular to the peptide plane and σ_{33} in the peptide plane with a σ_{33}/N−H projection angle of 20°). With these assumptions the approximate orientation of the (acetyl-CH$_3$)−N′ dipole vector in the ^{15}N CSA principal axis system is given by the Euler angles $\Omega = \{0, -64°, -180°\}$. All numerical simulations in (c) were performed using the SIMPSON simulation software.[77]

of ^{13}C coherences and since the first-order effective ^{13}C−^{15}N dipolar coupling and ^{15}N CSA Hamiltonians commute, to this order of approximation the ^{15}N CSA has no effect on the dipolar dephasing.[30] Therefore, the deviations from ideal behavior observed for the different *xy*-type phasing schemes with

increasing ^{15}N CSA must be due to higher-order terms in the effective Hamiltonian expansion.[64,65]

Conclusions

We have described a magic-angle spinning NMR experiment, which enables accurate internuclear ^{13}C−^{15}N distance measurements in uniformly ^{13}C,^{15}N-labeled solids. In multispin systems, the extraction of weak ^{13}C−^{15}N dipolar couplings using nonselective recoupling experiments is complicated by multiple ^{13}C−^{15}N and ^{13}C−^{13}C spin−spin interactions. The frequency selective REDOR technique presented here is based on a simple principle: a ^{13}C spin−echo is generated in a frequency selective fashion by a pair of selective π pulses applied to a ^{13}C−^{15}N spin pair in the center of the dipolar evolution period. The intensity of the ^{13}C spin−echo is modulated only by the dipolar coupling to the selected ^{15}N; the remaining ^{13}C−^{15}N dipolar couplings and ^{13}C−^{13}C scalar couplings involving the selected ^{13}C are refocused. With efficient proton decoupling and the use of well-compensated π-pulse phasing schemes, the spin dynamics can be described by the analytical expression for dipolar dephasing in an isolated heteronuclear spin pair under conventional REDOR, and the extraction of the ^{13}C−^{15}N dipolar coupling of interest is straightforward. We have demonstrated the utility of the experiment for accurate internuclear distance measurements in several U-^{13}C,^{15}N-labeled systems; in the model tripeptide, *N*-formyl-L-Met-L-Leu-L-Phe, a total of 16 ^{13}C−^{15}N intramolecular distances in the 2.5−6 Å range were determined with ∼0.1−0.3 Å precision.

The selective recoupling in FSR relies on ^{13}C and ^{15}N chemical shift resolution, and the technique is expected to greatly benefit from high static magnetic fields and high MAS frequencies. However, even under optimal conditions the measurements of multiple ^{13}C−^{15}N distances involving most backbone ^{15}N in U-^{13}C,^{15}N-labeled biological macromolecules, where spectral overlap can be quite severe, are expected to be challenging. Nevertheless, some potentially promising applications of the technique to systems of biological interest include ^{13}C−^{15}N distance measurements in the active site of multiply labeled proteins and structural investigations of peptide aggregates and molecules present at interfaces (e.g., U-^{13}C,^{15}N-labeled peptide bound to a protein).

Supporting Information Available: Two-dimensional ^{13}C−^{13}C and ^{13}C−^{15}N correlation spectra used to obtain ^{13}C and ^{15}N chemical shift assignments for [U-^{13}C,^{15}N]*N*-acetyl-L-Val-L-Leu and tables with selected intermolecular C−N distances in *N*-acetyl-L-Val-L-Leu and *N*-formyl-L-Met-L-Leu-L-Phe-OMe (PDF). This material is available free of charge via the Internet at http://pubs.acs.org.

JA003266E